UNIVERSITÀ
DEGLI STUDI
DI PADOVA

Sede Amministrativa: Università degli Studi di Padova

Dipartimento di Farmacologia ed Anestesiologia

"Egidio Meneghetti"

SCUOLA DI DOTTORATO DI RICERCA IN: Scienze Farmacologiche

INDIRIZZO: Farmacologia Molecolare e Cellulare

CICLO: XXIV

Alveolar surfactant phosphatidylglycerol, disaturated phosphatidylcholine, and SP-B kinetics in infants and adults with stable isotopes tracers, and H^+V-ATPase activity in B1 subunit knockout mice.

Direttore della Scuola: Ch.mo Prof. Pietro Giusti

Coordinatore d'indirizzo: Ch.mo Prof. Pietro Giusti

Supervisore: Dott.ssa Paola Elisa Cogo

Dottorando: Dott. Luca Vedovelli

Table of Contents

Chapter One
The Alveolar Surfactant System p. 7

Chapter Two
Stable Isotopes Tracers p. 21

Chapter Three
Lipids Metabolism:
Disaturated Phosphatidylcholine and Phosphatidylglycerol p. 29

Chapter Four
Protein Metabolism:
Disaturated Phosphatidylcholine and Specific Protein B p. 45

Chapter Five
Preliminary Study on the Role of H^+ V-ATPase Proton Pump p. 57

This work is dedicated
to the memory of
my father Fabio and
my friend John.
You will always be missed.

OVERVIEW

Alveolar surfactant is the key physiological structure that every mammal utilizes to live while breathing air. It is a mixture of proteins and lipids that lines the external part of the alveoli and allows a water-based organism to use air as source of oxygen. Disorders in surfactant's metabolism are known to be involved in life-threatening diseases like the acute respiratory distress syndrome and cystic fibrosis. In this thesis we describe the kinetics of two main surfactant's phospholipids (phosphatidylglycerol and disaturated-phosphatidylcholine) and of its specific protein B, *in vivo* in humans, all obtained with stable isotopes infusion protocols in children (phospholipids) and adults (protein SP-B). In the last part we tried to use the model of renal intercalated cells to approach the role of pH in the secretion of surfactant.

RIASSUNTO

Il surfattante alveolare è la struttura fisiologica che viene utilizzata da ogni mammifero per vivere e respirare in atmosfera. Si tratta di un complesso di proteine e lipidi che si trova nella parte esterna degli alveoli, dove svolge la sua funzione fisiologica permettendo lo scambio gassoso tra organismo (principalmente acquoso) e aria. Alterazioni del metabolismo del surfattante sono note in numerose e gravi malattie, come la sindrome da distress respiratorio e la fibrosi cistica. In questa tesi sono descritte le cinetiche di due principali fosfolipidi (fosfatidilglicerolo e fosfatidilcolina disatura) e di una proteina specifica del surfattante (SP-B), misurati *in vivo* nell'uomo attraverso l'infusione di isotopi stabili. Nell'ultima parte è descritto il tentativo di utilizzare il modello delle cellule intercalate del rene per studiare il ruolo delle variazioni di pH nella secrezione del surfattante.

Chapter One

The Alveolar Surfactant System

INTRODUCTION

Lungs hold a unique place among other organs. They allow gas exchanges between the water-based organism and the air and, at the same time, they protect the inside of the body from the external environment that they face directly. These fundamental features of the lungs are due to a tiny monolayer of lipids and proteins called alveolar surfactant.

SURFACTANTS PHYSICS

Surfactants are defined as molecules that have an "energetic preference" for the gas-liquid interface. An interface is the theoretical two-dimensional line between two phases, and phases are a confined amount of space that has the same physical properties.

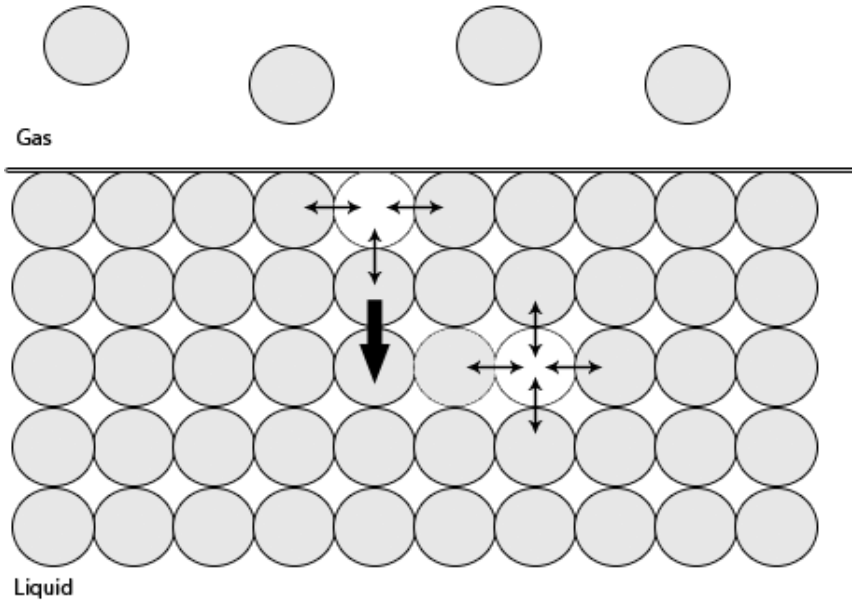

Figure 1. *Surface tension.* Gas molecules exert less attraction toward interface molecules. Resultant force for bulk molecules is zero but for surface molecules it is not and it act toward the bulk producing an opposing force to the expansion of the surface.

Molecules on the interfacial region of phases exhibit special behavior because the interaction between molecules at the edge of the phase is different from the interactions occurring in its bulk part. In the lungs the two phases are represented by the inner aqueous phase and the outer gas phase. In the bulk of the aqueous phase, molecules are subjected to the same attraction in all direction by their nearest neighbors but at the interface with air, gas molecules attraction is trivial (Figure 1). The negligible attraction toward one direction creates an unbalance in attractive forces leading to a resultant force inward the liquid phase (because surface molecules seek a minimal area), generating surface tension. Surface tension is a thermodynamically measurable force expressed like the variation of Gibbs free energy for a unit of area (surface) at constant temperature, pressure and number of moles.

$$\sigma = (\delta G/\delta A)_{T, P, n}$$

Surface tension could be seen as a measure of the work necessary to increase the surface area of a system.

Surfactants are molecules that always lower surface tension and they all share characteristics to be amphipatic and to form a monolayer at the gas-liquid interface with the polar part toward the aqueous phase and the non-polar edge toward the air. Surfactants reduce the imbalance between attractive forces at the interface because the attraction of surfactant's molecules by liquid molecules is less than the attraction of liquid molecules for each other. Surfactants' behavior depends on some physical and chemical properties of the system (i.e. temperature, chemistry, concentration) but their power to lower surface tension depends also on how rapidly they are compressed. More rapid is the rate of compression, less is the final surface tension. In the lungs, this is due mainly to dipalmitoyl phosphatidylcholine (DPPC, the most surface-active component of alveolar surfactant) that, when compressed, forms a highly packed solid-like monolayer, responsible of the surface tension reduction. Finally, packing of the monolayer allows phospholipids with less affinity for the interface (they have more free energy) to be *squeezed out* from the film, modifying the concentration

of some phospholipids (increase of DPPC concentration) thus enhancing even more the surface tension reducing properties of the surfactant [1].

ALVEOLAR SURFACTANT

Alveolar surfactant is the mixture of lipids and proteins that lines the external part of the 120 m^2 surface of alveoli in the lungs. It allows the normal breathing cycle lowering the surface tension on the alveoli's edge during expires. Alveolar surfactant is only produced by alveolar type II cells that, with alveolar type I cells and macrophages, are the three types of cells found in the alveolus (Figure 1). Type I cells (or pneumocytes I) are the main population representing the 95% of total epithelial cells. They are finally differentiated cells that serves nearly only as a barrier between blood and air. Type II cells (or pneumocytes II) accounts the other 5% of epithelial cells. They are the stem cells of the alveolar epithelium and they can divide in Type I cells in response to physiological or pathological stimuli. Alveolar macrophages play a crucial role in host defense, surfactant catabolism and alveoli remodeling. The role of alveolar macrophages will be discussed later in this chapter.

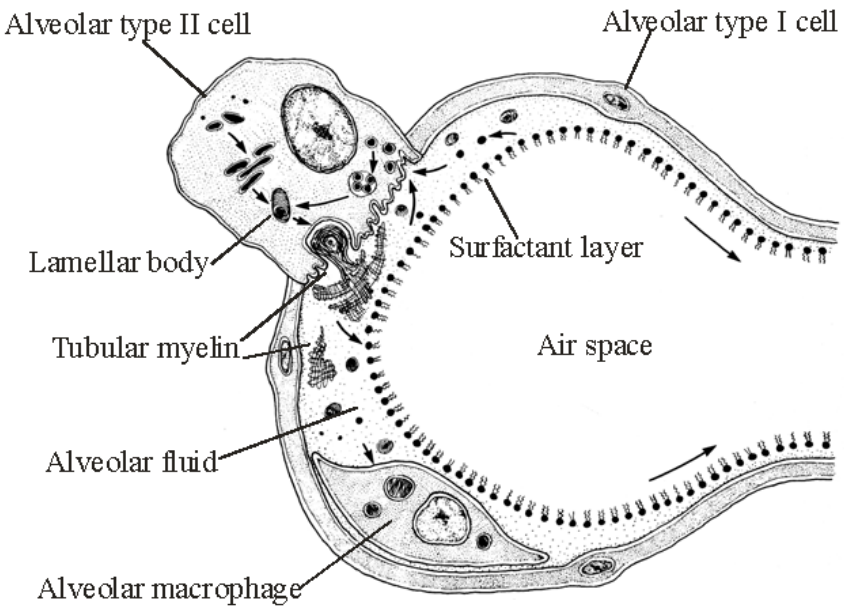

Figure 2. *The structure of the alveolus.* Tubular myelin is the form in which surfactant is secreted by Type II cells before spreading in a monolayer (adapted from Hagwood *et al.* [2])

The function of surfactant as a surface-active agent is mainly due to its phospholipids' composition (Table 1).

Phospholipids Class	Cell-free Lavage	Lamellar Body Isolates
PC	80.0 ± 0.9	77.4 ± 0.2
PG	6.8 ± 1.4	8.9 ± 1.3
PI + PS	5.4 ± 1.3	4.7 ± 0.6
PE	3.7 ± 0.4	5.0 ± 0.9
SPH	2.1 ± 0.4	1.8 ± 0.7

Table 1. *Average content of phospholipids from lavage and lamellar bodies isolates.* Data are averages for six lavage studies and four lamellar bodies studies involving different animal species and different ages[3]. See text for abbreviations.

Among these phospholipids (PL) the most powerful in lowering surface tension is DPPC that represents alone nearly one third of the total PL content of the alveolar surfactant. Endogenous surfactant also contains anionic (phosphatidyl-glycerol PG, phosphatidyl-inositol PI and phosphatidyl-serine PS) and zwitterionic (phosphatidyl-ethanolamine PE and sphingomyelin SPH) phospholipids. The presence of atypical PL classes as disaturated PC (DSPC) and PG is a characterizing and intriguing feature of alveolar surfactant. In fact, DSPC is uncommon in mammalian membranes and PG is barely present in mammalian tissues while common in bacteria and plants.

Surfactant's specific (SP-) proteins (6-8% of total surfactant) are four (A to D) and participate to surfactant's formation and functions. SP-A influences (together with SP-B and calcium) and enhances the aggregation of PL[4,5] in a variety of "large aggregate" forms. The most important of these is tubular myelin, a lattice-like tubular structure. Tubular myelin is the form that surfactant assumes just after being excreted from Type II cells and just before being adsorbed as a monolayer[6,7]. While SP-A gene knockout is compatible with life in a mouse model [8], SP-A-free lung extracts ability to resist to plasma proteins inactivation is enhanced by the addition of SP-A[9]. SP-B and SP-C are small hydrophobic apoproteins that have extensive molecular interactions with PL and a striking impact in enhancing adsorption and surface reducing power of the surfactant. The addition of SP-B/C to DPPC enhances the adsorption of this

PL *in vitro* near to the physiological level and much more than DPPC alone[10]. SP-B/C accomplish the facilitation of adsorption disrupting and fusing PL bilayers and selectively enhancing the insertion of specific PLs into vesicles and surface films. SP-B seems to be the more active between the two proteins[11]. SP-D represents a separate group of surfactant proteins. It shows structural similarities with SP-A but despite being both members of the C-type lectins family, only SP-A shows surface-active properties, while SP-D participates only to the host defense response agglutinating carbohydrates and participate to surfactant metabolism[12-14]. For the role of SP-D in surfactant catabolism, see the following sections.

SYNTHESIS AND MATURATION

Alveoli and surfactant appears during the "canalicular period" of the embryonic development that, in humans, goes from the 17th to the 28th week of gestation. The amount of surfactant required for alveolar stability to support gas exchanges is produced between weeks 24th to 26th thus preterm infants born near this period requires the administration of exogenous surfactant (usually from swine o bovine origins) to lessen mortality and morbidity[15].

Inside the alveolus, Type II cells are the main site for synthesis and metabolism of surfactant PL and proteins. Type II cells could synthesize *de novo* surfactant components, catabolise or reuse them to form new surfactant[16]. PL and proteins are synthesized in the endoplasmatic reticulum and transferred via vesicles trafficking from the Golgi to specific lysosome-like organelles called "lamellar bodies" where surfactant is stored prior to secretion into the alveolus lumen. During the transfer from the Golgi and inside the lamellar bodies, surfactant components reach their mature state through post-translational modification of proteins and precise assembly of PL[17,18].

The synthetic pathway of PL is similar to the other cells and tissue but alveolar cells are specialized to give rise to a PL population enriched in monoenoic and disaturated phosphatidylcholines. PC is synthesized *de novo* by the CDP-choline incorporation pathway as in other cell types (with choline-phosphate cytidylyltransferase as a pivotal regulatory enzyme) but what is not common in other cells, the disaturated PC, is thought to be formed by a remodeling pathway that converts monoenoic PC to disaturated PC[19,20].

DSPC, PG and PI are known to have linked synthesis pathways in rabbits' Type II cells but the quantitative contribution of each of these pathways remains a speculation. It was demonstrated[21,22] that an increase of PC synthesis in late gestation is accompanied by an increase of the PG content in Type II cells due to an intracellular increase of cytidine monophosphate (CMP) and a consequent stimulation of the reverse reaction that forms PI. More specifically, PI holds the same precursor of PG, cytidine diphosphate diacylglycerol (CDP-diacylglycerol). When the CMP level rises, the reverse reaction of PI formation takes place forming CDP-diacylglycerol that is available for PG's synthetic pathway that ends with an irreversible reaction, rising in this way the content of PG in alveolar surfactant (Figure 3)[23].

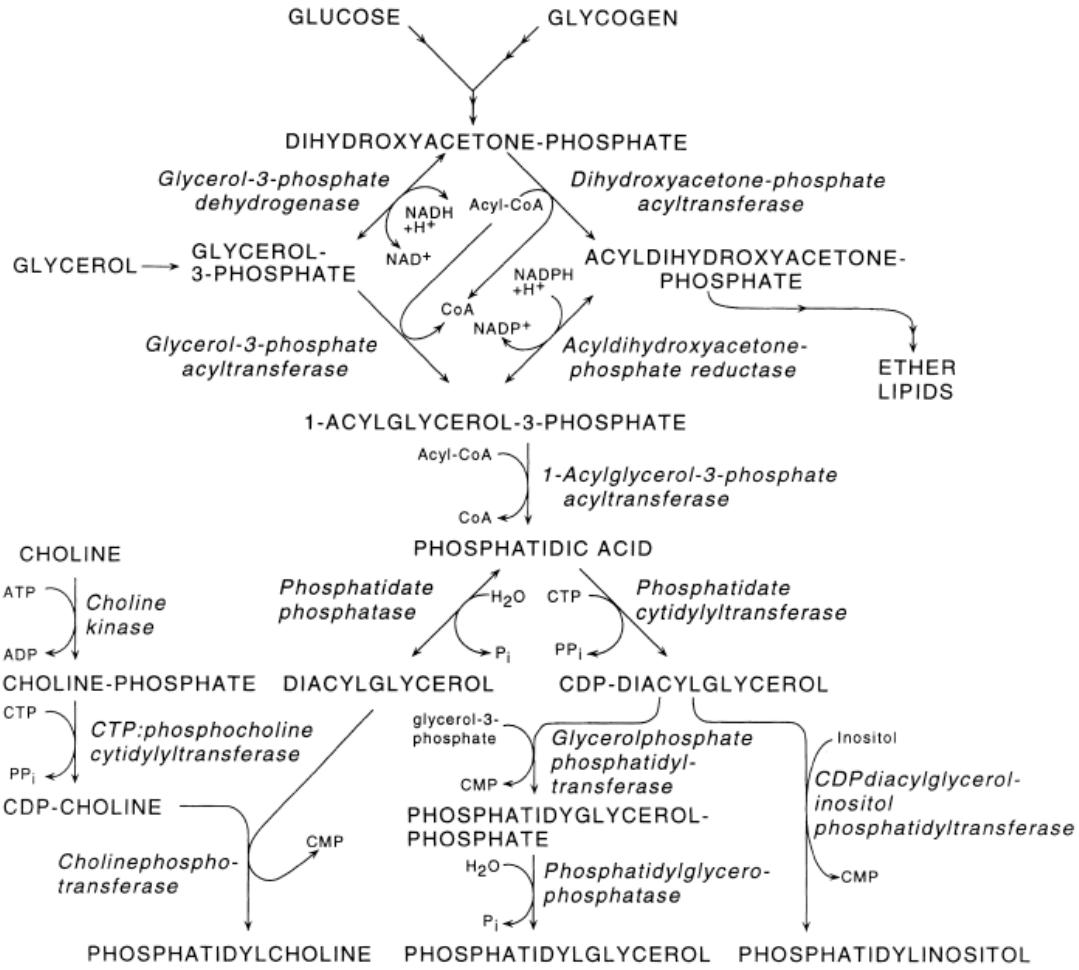

Figure 3. *Biosynthesis of phosphatidylcholine, phosphatidylglycerol and phosphatidylinositol*[24].

Surfactant proteins can be all synthesized in Type II cells but only SP-C seems to be synthesized only in Type II cells. SP-A, B and D could be synthesized in other locations of the lung, for example in Clara cells, where they take part to the regulation of host defence[25,26]. Post-translational modifications affect especially SP-B that is deeply modified during the formation of mature lamellar bodies until reaching its mature form of 8.7 kDa[27].

A plethora of growth factors and hormones are linked to the surfactant synthesis and maturation but glucorticoids are the most interesting and most studied mediator, because of the observation that the administration of prenatal steroids 24-72 h before a premature birth, increases the content of surfactant and the maturity of the newborn's lungs[28]. Intriguingly dexamethasone inhibited type II cell proliferation *in vitro* but increased SP-B expression[29]. Moreover, surfactant synthesis and/or maturation is positively effected by adrenergic stimuli and cytokines[30,31].

SECRETION

Secretion of surfactant is a fine mechanism regulated probably entirely by factors external to the Type II cells[29]. Secretion rate is faster than surfactant synthesis so internal mechanisms to recover and reuse the depleted molecules should take place to avoid the surface tension to rise[32]. In fact, radio-labeled palmitic acid is incorporated in surfactant's PC within minutes from the injection but it appears at the alveolar level at least 12 h later[33]. Physiologically, surfactant level rise and, consequently, lamellar bodies diminish, even after a single deep breath and, in the same way, physical exercise is known to increase 14-fold surfactant level in swimming rats[34,35]. All the stimuli that increase cAMP have the effect of increasing secretion. Examples are beta-adrenergic agents, methyl xantines, forskolin and cholera toxin, probably involving protein kinase A and C pathways. The most powerful *in vitro* secretagogues known are ATP and tetradecanoylphorbolacetate (TPA) and they act through calcium mobilization and PKA activation[36]. Calcium is a fundamental actor in secretion, involved as second messenger in almost all the secretory stimuli.

The proposed mechanism of action of secretion involves a sustained release of calcium into the cytoplasm that is necessary for both maturation and exocytosis of surfactant vesicles (Figure 4). Moreover calcium seems to be the messenger able to couple mechanical stretch and secretion maybe trough the release of ATP

after lung overexpansion or, conversely, mechanical stretch could increase the diameter of pores used by lamellar bodies to fuse with the plasmatic membrane of Type II cells[31].

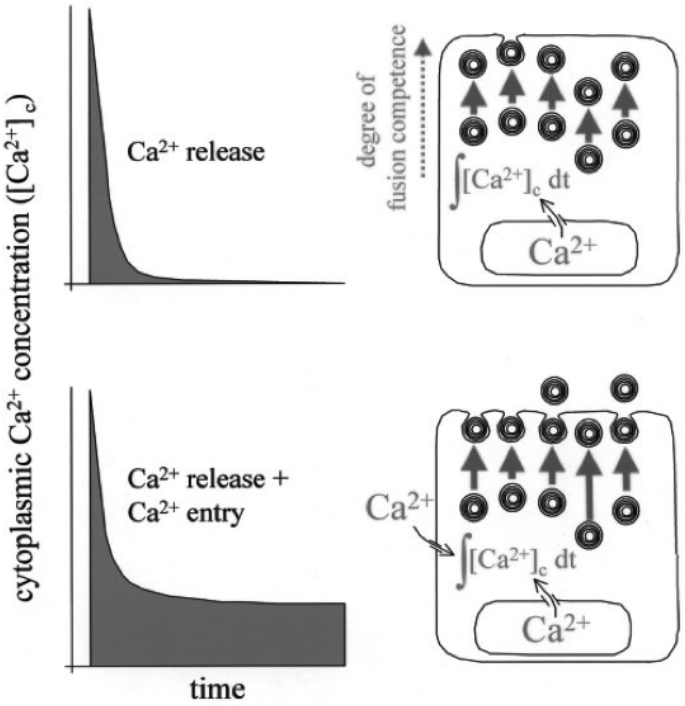

Figure 4. *Proposed model of biphasic, calcium-mediated, secretion of alveolar surfactant.* Calcium promotes maturation and secretion of surfactant vesicles when the stimulus is maintained over the time. From Dietl P. *et al.* [31].

Intracellular alkalosis stimulates secretion but variations of the extracellular pH do not affect exocytosis of surfactant[37,38]. It was demonstrated recently that secretagogues (ATP and PMA, a phorbol ester like TPA) act dissipating the pH gradient of lamellar bodies (that have a low pH that is crucial for the processing of SP-B, SP-C and lipid oraganization[39,40]) disrupting the assembly of the proton pump H^+V-ATPase in a calcium dependent fashion[41].

Regarding inhibition of secretion, the whole surfactant and its lipids are able to inhibit surfactant secretion[42] but the most interesting role is played by SP-A that inhibits secretion while enhancing reuptake of PL into alveolar Type II cells[43]. It was proposed that SP-A's inhibition of secretion is linked to his lectin-like conformation[44] but more recently it was showed that SP-D (that is lectin-like surfactant protein as well) counteract the inhibitory effect of SP-A[45]. Other secretagogues (e.g. isoproteronol or terbutaline) enhances both secretion

and clearance of PL[46], but SP-A seems to act influencing a more sustainable way of using surfactant, slowing the secretion during the early stages of the process until enough material entered the cell by the SP-A-mediated uptake process. Inhibition of secretion was observed also blocking some cytoskeletal elements using colchicine and vinblastine. The secretion blocked in this way was not restored by adding secretagogues [47,48].

RECYCLING AND CATABOLISM

After serving onto the alveolar surface, surfactant lipids and proteins have three destinies: (1) being reused without degradation; (2) partially or fully degraded and recycled; (3) removal from the surfactant system as catabolites or intact molecules. Recycling and catabolism are done directly by Type II cells and macrophages participate only to catabolise surfactant. Each cell type is responsible of the 50% of surfactant reuptake[49]. In the alveolar milieu macrophages are in the alveolar space ("alveolar macrophages", recovered with the bronchoalveolar lavage fluid, BAL) or they are associated with lung tissue. Macrophages are unable to recycle surfactant into its active form, so, when internalized, surfactant components are degraded and released in extracellular compartments[50]. Inhibition of the activity of both types of lung macrophages by different factors lead to a concentration of saturated PC four to eight times greater, while the synthesis and secretion were demonstrated unchanged in respect to normal mice. Increase of surfactant amount was determined to be due to a defect in catabolism by alveolar macrophages[51-53].

Type II cells internalize surfactant components in a more selective way than macrophages. Among anionic ferritin, cationic ferritin, 70kDa destran and colloidal carbon, only cationic ferritin is taken up by Type II cells[54]. Lipids re-incorporation into lamellar bodies was demonstrated *in vivo*[55,56] and *in vitro*[57] in isolated cells. Moreover, SP-A stimulation of surfactant uptake is cells specific to macrophages and Type II cells. Lung fibroblasts are not affected[43]. Some evidences support the presence of high specificity receptor(s) in Type II cells[58]. SP-B and SP-C both enhances lipids uptake but the effects were not saturable and the effect may be related only to physical changes in liposomes than to a receptor mediated mechanism[59]. The role of SP-D on surfactant catabolism was unclear until a SP-D (-/-) mouse was crated[60]. Newborn SP-D deficient mice showed a normal surfactant ultra-structure but soon after birth a marked

accumulation of surfactant was observed both in tissue and in into the alveolus. Synthesis and secretion were found normal, so SP-D deficiency impaired uptake, catabolism or recycling by Type II cells [61,62]. Uptake was observed to be reduced in knockout mice and a particular form of surfactant called "small aggregates" vesicles (that contains the surfactant that is going to be catabolized and/or recycled) were filled by lipids in an abnormally dense state (multilamellar vesicles). Normal surfactant ultra-structure was re-established adding SP-D to the BAL fluid from SP-D (-/-) mice. Thus, SP-D regulates surfactant metabolism influencing the ultra-structure of surfactant maybe interacting with PI and fatty acids[63, 64-67].

DYSFUNCTIONS

The surfactant homeostasis can be disturbed acting directly on the physical properties of the interfacial film or on its chemical composition (Table 2). Plasma and blood proteins (albumin, hemoglobin, fibrinogen and fibrin) leaking into the alveolar space after a defect of the lining epithelium, give the major contribution on inhibition of the surface tension lowering properties of the surfactant and/or the interference on its adsorption to the alveolar surface. The mechanism of action of these proteins is hided inside the intrinsic chemical composition of the protein itself. Every protein has a certain degree of polarization having parts showing a more polar attitude than the others, thus every protein has a degree of surface activity. Plasma proteins leaking into the alveolus are not as effecting as surfactant in lowering surface tension so they inhibit competitively the surfactant function.

Physical Inhibitors
Plasma and blood proteins
Meconium
Cholesterol
Lysosphospholipids and unsaturated cell membrane phospholipids
Biochemical Inhibitors
Reactive oxigen species
Lytic enzymes (proteases and phospholipases)

Table 2. *Endogenous inhibitors of surfactant.*

The effect of these proteins depends on the concentrations ratio "surfactant-to-protein". Smaller is the ratio, more is the damage made by the protein on the surfactant film, so the inactivation could be mitigated or ended by raising the concentration of surfactant. Lysophospholipids, cholesterol and PL from the cell membranes, act in a similar way but penetrating directly into the film and fluidizing it, limiting its physiological properties.

Proteases (e.g. elastase and phospholipases) are released during inflammation and while chemically degrading surfactant, they create a vicious circle that let degradation products to further activate the immune system. Reactive oxygen species are also a side product of immune system activation that can attack PL and surfactant proteins.

Meconium (the first fecal product of the newborn) could be expelled before birth following a distress (e.g. perinatal asphyxia) and thus being inspired into the lungs with the amniotic fluid. Meconium complex composition probably acts on the lungs with a combination of mechanical inhibitions and chemical/biological stimulation of inflammation[68-70].

DISEASES

Dysfunction and inactivation of surfactant lead, or are the consequences, of the respiratory distress syndrome named RDS (or NRDS) in premature infants, or acute (formerly *adult*) respiratory distress syndrome (ARDS) in term babies and adults. Acute lung injury (ALI) presents the same clinical definition of ARDS but in a milder extent.

Lungs are the organs that determine the survival of preterm infants within the 24th to the 32nd week of gestation. RDS affects 50,000-60,000 infants every year in the United States and it was the mayor cause of neonatal mortality in the developed countries before the 1990's[71] and it still remains a major cause of infant illness even if surfactant replacement therapies improved significantly the outcome of preterm babies. RDS rate of incidence depends on the gestational age and on the weight (<1,500 grams) of the preterm infant. More than 50% of babies develop RDS if the gestational age is less than 29 weeks. The incidence decrease to 5-10% after the 35th week[72]. RDS was initially named *hyaline membrane disease* (HMD) because of the protein-rich, shiny appearance of alveoli and small airways found in preterm infants died for

respiratory distress. Avery and Mead proved a direct connection between HMD, RDS and surfactant dysfunction in a fundamental work in 1959[73]. Nowadays is well established that the cause of RDS is a lack of surfactant due to an immature population of Type II cells. As mentioned before, surfactant production starts between the 24-26th weeks of gestation but the minimum level for normal breathing is reached around the 32nd week. Clinical characteristics of patients with RDS are showed in Table 3 [74].

- Alveolar collapse (atelectasis)
- Decreased compliance (difficulties to inflate)
- Alveolar overexpansion (to overcome atelectasis of the other parts of the lung)
- Intrapulmonary shunting (impaired ventilation/perfusion)
- Hypoxemia
- Hypercapnia (thus, acidosis)

Table 3. *Clinical characteristics of RDS.*

The course of RDS, in the best scenario, resolves typically in 2-5 days with minor interventions like oxygen therapy and a mild positive pressure (i.e. nasal continuous positive air pressure, CPAP) because of a fast development of Type II cells due to hormones and other grow factors released after birth. When clinical interventions are ineffective, the patient goes toward a marked hypoxemia despite intensive mechanical ventilation and oxygen therapy. The final result is a diffused atelectasis with the concurrent overexpansion of the neighbors parts[75].

ARDS and ALI are the inflammatory, pulmonary reflection of a variety of causes that can origin from every organ in the body. Incidence of ARDS is variable depending on the parameters used to define the disease but 50,000 – 150,000 patients are affected every year in the United States and mortality in about 50% despite advanced in clinical care. The American-European Consensus Committee defined ARDS and ALI as in Table 4[76].

1. Acute onset
2. PaO_2/FiO_2 (arterious oxygen tension / fraction of inspired oxygen) ≤ 200 (regardless of positive end expiratory pressure, PEEP).
3. Bilateral infiltrates on frontal chest radiography
4. Pulmonary capillary wedge pressure ≤ 18 mmHg (if measured) or no evidence of left atrial hypertension.

ALI has the same clinical definition but with a less severe PaO_2/FiO_2 of ≤ 300.

Table 4. *Clinical diagnosis of ARDS/ALI.* As defined by the The American-European Consensus Committee.

The most common causes of ARDS for adults are sepsis, mechanical trauma (also head injuries), multiple transfusions, and gastric aspiration. For children common causes are sepsis, near drowning, hypovolemic shock, and closed space burn injury[77-79]. The onset of the disease follows all the routes of inactivation of surfactant described before (biophysical, chemical degradation and, chemical interaction). The damage of Type II cells coming from the inflammatory activation effects synthesis, packaging, secretion and metabolism of surfactant[80].

RATIONALE

After the presented premises, understanding how the surfactant system reacts to insults is an intriguing question with evident clinical significance. In this thesis we measure the kinetic behavior of SP-B in ARDS patients to map the changes in surfactant synthesis and metabolism during the inflammatory activation. Moreover we measured simultaneously the kinetics of DSPC and PG in patients with various lung diseases to understand if the destiny of the two PL is the same or metabolism of surfactant is regulated in someway toward a specific PL. Finally, an insight toward the regulation of secretion was made trying to indentify the role of acid-base balance in surfactant metabolism.

Chapter Two

Stable Isotopes Tracers

PRINCIPLES

In the elements classification by the periodic table every occurring species with the same number of protons (atomic number) but different number of neutrons (different mass number) occupy the same place in the table. For every element, each species that differs for the mass number but not for the atomic number is called isotope (from the Greek, "at the same place"). Some isotopes undergo to a radioactive decay and they are known as *radionuclides*. For other isotopes, decay have never been seen and so they are called *stable isotopes*. For each element a natural-occurring variable number of stable isotopes is observed. For example hydrogen have three main isotopes (Figure 1): protium (the "classic" and most abundant form of hydrogen with one proton and no neutrons), deuterium (stable, with one proton and one neutron), and tritium (radionuclide, with one proton and two neutrons).

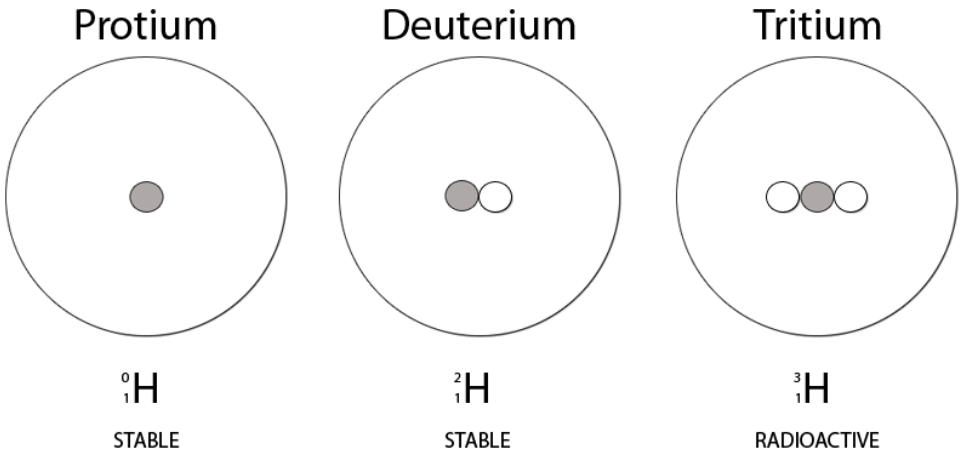

Figure 1. *Hydrogen isotopes.*

Only hydrogen isotopes have each a different name, for isotopes of other elements they are called referring to the superscript that indicates the mass number. For example ^{13}C (subscript is often avoided) is called "carbon thirteen".

Because of their chemical behavior is the same, isotopes can be used in biological science to discriminate or "trace" molecules, incorporating them in natural occurring components and so trace their route into the body. Radioactive isotopes are still used in animal models for their easiness of detection but they are clearly not suitable for human use. With the availability and develop of mass spectrometry techniques today is possible to discriminate two molecules by their atomic mass even if they have the same chemical behavior and reactivity. Stable isotopes tracing is inserted in this scenario, allowing researcher to trace components of the human body in an ethically sustainable way, without interfering with the homeostasis or with the clinical practice. An example of well established clinical use of stable isotopes as diagnostic tools is detection of *Helicobacter pylori* with ^{13}C-urea. *Helicobacter p.* can metabolize urea because of urease synthesized only by the bacteria and not from the human host so ^{13}C-CO_2 can be detected in the breath if the bacteria is present[81].

MASS SPECTROMETRY

A mass spectrometer is basically an instrument to measure the weight of a substance at molecular level. It consist in three components:

1. *The Ion Source*. Where the molecules are reduced into ions.
2. *The Analyzer*. Which separates the generated ions based in they mass-to-charge (*m/z*) ratio.
3. *The Detector*. That amplifies and digitally converts the molecule signal (usually it is an electro-multiplier).

Ion Sources are of different types but their role is to let the neutral molecules to become charged ions so they can interact with the electromagnetic field of the Analyzer and be separated.

$$M + e^- \rightarrow M^+ + 2e^-$$

The two most common types of ion sources are Electron Impact Ionizator (EI) and Chemical Ionization (CI). EI uses an electron beam (usually 70 eV) to ionize the neutral molecule coming into the source. The advantage of EI is that for a given molecule at a given electron beam power, the ion fragmentation pattern is consistently characteristic of that particular molecule. CI uses ionized gas with a small molecular weight (e.g. methane or ammonia) to ionize the analyte. In respect to EI the ionization is milder (sometimes required for fragile molecules that can not sustain an harsher ionization), can be done with positive and negative ions, but the fragmentation pattern is not as consistent as in EI. More ion sources are available and useful, like the electrospray ionization (ESI) for liquid samples, but only the first two were used for this research.

Analyzers are also of different types but their common goal is to separate charged molecule. The oldest but still reliable analyzer is a curved electromagnet (Figure 2).

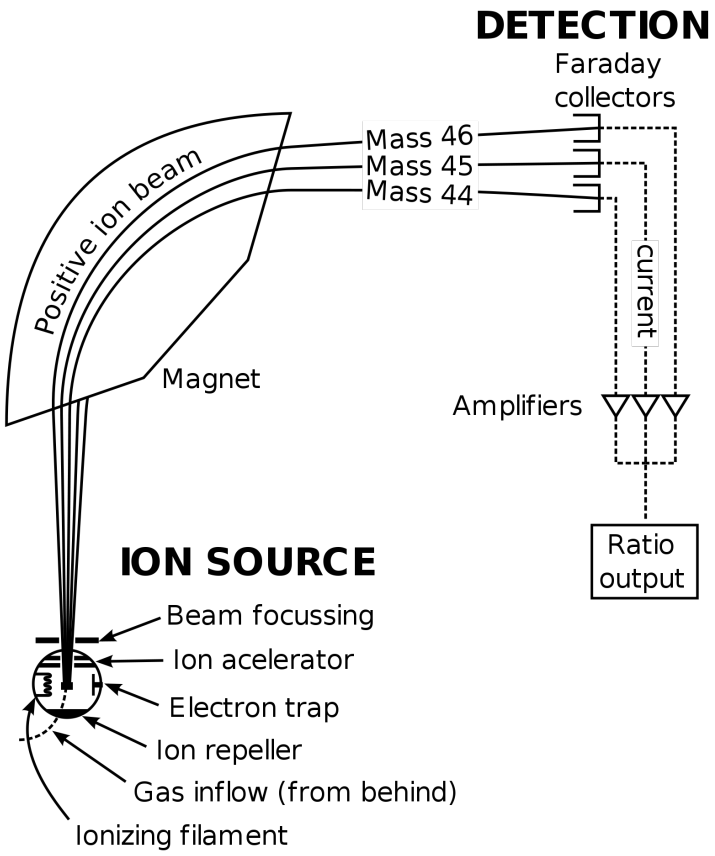

Figure 2. *Schematic representation of a mass spectrometer.* Despite being the first configuration of a mass spectrometer, is still reliable and used today in Isotope Ratio Mass Spectrometers (IRMS).

When ion fragments exit the ion source, they enter the analyzer and they are deflected more or less depending on their mass-to-charge ratio. Higher is the m/z less they will be deflected. Another widely used analyzer is the "quadrupole" analyzer (Figure 3).

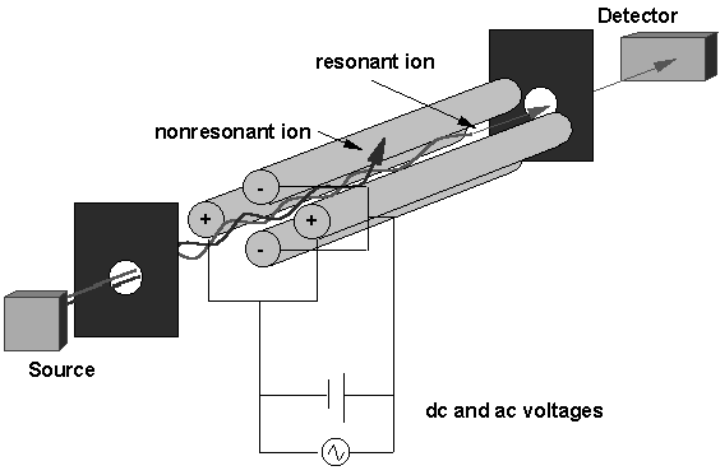

Figure 3. *Schematic representation of a quadrupole.* Modified from a drawing of Brian M. Tissue (VirginiaTech).

A quadrupole is composed by two pairs of metal rods. Each rod pair is connected electrically: a constant dc current is applied to the four rods and a radio frequency voltage (RF) is applied between one pair of rods and the other. Modulating the RF voltage (and so the oscillating field) the quadrupole is able to select a specific m/z ratio and thus specific ions. Ions resonant with the field will pass trough and reach the detector, and non-resonant ions will not.

Detectors are usually electromultipliers and Faraday's cups (Figure 4). Faraday's cups are made of a conductive material and they are designed to give an electron current when a charged molecule hits the cup.

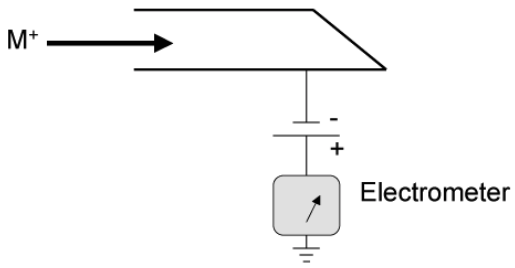

Figure 4. *Schematic representation of a Faraday's cup.*

ISOTOPE RATIO MASS SPECTROMETRY

IRMS is an application of mass spectrometry that permits to measure slightly differences between samples isotopic abundances. Magnetic analyzer is used as analyzer because of its extreme stability that permits a very precise measurement of isotopes ratios, even natural occurring differences. The limitation is the number of ions that can be monitored that is consequently limited by the number of cups. Each cup can monitor a single ion, or better, a single m/z ratio. In an IRMS, first of all, the organic sample is pyrolised to its fundamental components H_2O, CO, CO_2 and H_2, then water is removed and the sample sent to the ion source (EI type) and finally trough all the instrument. As an example, as showed in Figure 2, isotopic ratio is calculated from simultaneous measurement of 44 m/z $^{12}CO_2$ and 45 m/z $^{13}CO_2$. Isotopic enrichment of the sample has to be compared to a standard (Table 1). Ratios are usually expressed as *delta* that represents the variation (part per thousand) of the isotopic ratio of the sample.

$$\delta X(‰) = \left(\frac{R_{sample} - R_{standard}}{R_{standard}} \right) x\,1000$$

Where R= heavy isotope mass/ light isotope mass ratio (i.e. $^{13}C/^{12}C$, $^{2}H/^{1}H$); $\delta X>0$ when the heavy isotope is enriched versus the standard; $\delta X<0$ when the light isotope is enriched versus the standard[82].

Element	Stable isotopes	Natural abundance (%)	Standard ratio values	International standard reference
Hydrogen	^{1}H ^{2}H	99.985 0.015	$^{2}H/^{1}H$= 0.000316	VSMOW (Vienna Standard Mean Ocean Water)
Carbon	^{12}C ^{13}C	98.892 1.108	$^{13}C/^{12}C$= 0.0112372	PDB (Pee Dee Belemnite)
Oxygen	^{16}O ^{18}O	99.7587 0.2039	$^{18}O/^{16}O$= 0.0039948	VSMOW (Vienna Standard Mean Ocean Water)

Table 1. *Principal stable isotopes used in biology.* Belemnite is a fossil $CaCO_3$

STABLE ISOTOPES TOXICITY

High deuterium doses showed toxic effects in animal studies. A 10-20 % of deuterium in total body fluid causes an alteration in cellular function, decrease in protein synthesis and enzymatic reaction rate (some enzymes can discriminate between isotopes). Then, a 30-40 % of deuterium in total body fluid is fatal. In human studies doses are much lower ranging from 1 to 80 mg/kg of body weight with a LOAEL (Lowest Observed Adverse Effect Level) to be about 200-400 mg/kg of body weight. For carbon, unlike deuterium, ^{12}C and ^{13}C have lower mass difference percentage (for deuterium is about 50%, for carbon is about 8%) and thus clinical relevant effects are unlikely to happen. In clinical studies, the usual tracer dose is 1-25 mg/kg of ^{13}C[83,84].

GAS CHROMATOGRAPHY

Until now we have spoken about how the molecule that arrives to the mass spectrometer is identified by its mass-to-charge ratio but enrichment is better analyzed if only one compound at time enters the mass spectrometer. This is a not a absolute requisite for a mass spectrometer in general but is mandatory for the IRMS where all compounds are reduced to the same small ions. A reliable on-line method to separate compounds prior to the mass spectrometry analysis is to pass the sample through a gas chromatographer (GC). Prior to GC the sample is volatilized (or "derivatized") adding a functional group to the analyte to lower its boiling temperature. The sample is then injected into a vaporization chamber (about 250°C) and carried into a separation column (25 to 100 meters long) with an inert gas (helium). In the column, samples interact with the stationary phase according primarily to their boiling point. Usually high boiling molecules interacts more with the column than low boiling molecules. In the meanwhile a ramp of temperatures is applied to the column and molecules starts to exit the column (and enter the mass spectrometer or another detector) depending on their strength of interaction with the column. Each exiting molecules generates an event (a peak in the chromatogram) that is recorded and plotted against time. A mass spectrometer and/or a standard can be used to identify the peak (Figure 5).

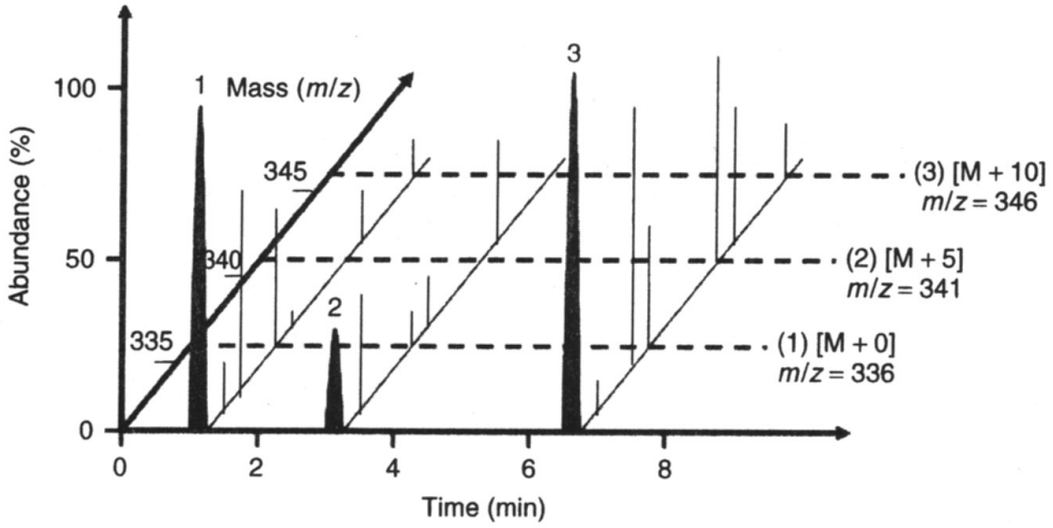

Figure 5. *Three-dimensional GC/MS chromatogram.* The first chromatogram (X and Y axes) shows the results of a GC run with three different peaks each representing an isolated molecule. Each molecule is then analyzed by the mass spectrometer and gives the fragmentation pattern, or "fingerprint", of the specific molecule.

STUDY DESIGN

In our previous studies we described the kinetic behavior of surfactant components with stable isotopes as tracers[85-94]. Here we administered deuterium to infants with various pulmonary diseases and to controls (under mechanical ventilation for causes not related to the lungs) to trace part of the lipid metabolism of DSPC and PG. In particular we developed a new method to isolate PG and DSPC with the necessary purity for a mass spectrometer analysis. This allows, for the first time, the simultaneous measurement of these two PL in the same sample[95] (Chapter 3). Then (Chapter 4) we used 1-^{13}C leucine to trace the synthesis of the protein SP-B, together with deuterium to trace DSPC, in adults hospitalized for ARDS[96].

Chapter Three

Lipids Metabolism: Disaturated Phosphatidylcholine and Phosphatidylglycerol

BACKGROUND

Alveolar surfactant is composed primarily of phospholipids (PL, 80-85% by weight), with a predominant presence of disaturated phosphatidylcholine (DSPC, about 50% of total PL). Neutral lipids represent 10% of total PL and specific surfactant proteins (SP) A, B, C and D represent together 5-10% of the alveolar surfactant. DSPC gives the major contribution, among PL, in lowering alveolar surface tension (Figure 1)[97]. Dipalmitoyl-phosphatidylcholine (DPPC) is the most abundant species of DSPC [98].

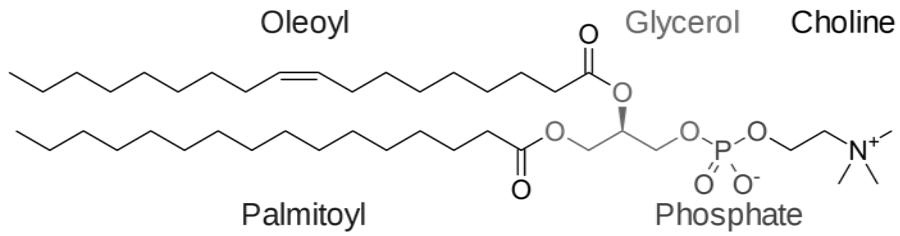

Figure 1. *Palmitoyl-oleyl-PC.* This is an example of a PC species. Saturated species (DSPC) contains two saturated residues. The most common saturated residue is the palmitate one.

PG is the third most abundant PL in airway's surfactant (5-15% of total PL) and its fatty acids consist primarily of palmitate (C16:0) and oleate (C18:1ω9) residues (Figure 2).

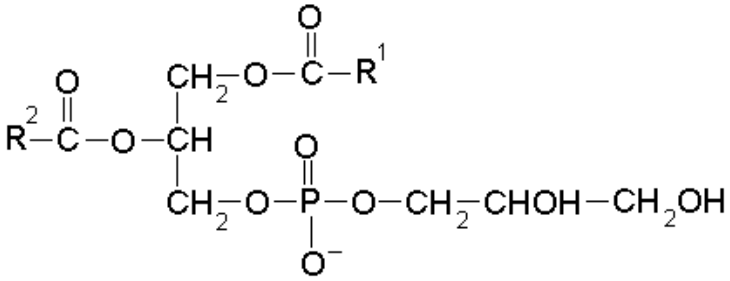

Figure 2. *Schematic representation of PG.* R^1 and R^2 are the two fatty acid residues. Even for PG we found that palmitate residue is the most abundant.

Clinically, DSPC and PG levels decrease in preterm infants respiratory distress syndrome (RDS), acute respiratory distress syndrome (ARDS, that affects term newborns and adults) and in cystic fibrosis[76,99]. Interestingly, patients affected with most severe forms of ARDS, showed a dramatic decrease of airway PG[100]. PG binds the hydrophilic etheropeptide KL-4 of surfactant specific protein B (SP-B) and the complex plays a crucial role in lowering surface tension by promoting the formation of surface-active pools beneath the monolayer that act as reservoirs of surfactant active materials readily available during alveolar expansion[101].

DSPC and PG synthesis requires free fatty acids derived from three possible sources: (1) fatty acids present in plasma in free form or derived from circulating lipoproteins; (2) fatty acids derived from surfactant PLs (recycling); and (3) fatty acids synthesized de novo by Type II pneumocytes or by liver cells with subsequent uptake by the lungs from serum lipoproteins. The relative contribution of the various sources of fatty acids is unclear and probably varies with gestational age, development, and nutritional status[102,103]. Interestingly, PG appears to be more susceptible than DSPC to changes in degradation and recycling[104,105].

In this study, we coupled the labeling of palmitate residues in PG and DSPC with deuterium derived from body water[106] (deuterium is administered to patients as deuterium oxide or deuterated water ^2H_2O) with the sensitivity of a gas chromatographer coupled with an isotope ratio mass spectrometer (GC-C-IRMS) to measure simultaneously the turnover from the alveolar space of palmitate-PG and palmitate-DSPC, in infants with normal and diseased lungs.

MATERIAL AND METHODS

Patient Enrolment

Patients (5 M, 3 F) were admitted to the Neonatal Intensive Care Unit, Department of Pediatrics, University of Padua, from 2002 to 2009. Informed consent was obtained from both parents. We enrolled 8 infants requiring mechanical ventilation: 6 for lung diseases and 2 for postoperative care or neurological failure (Table 1). Local Ethics Committee approved the study.

Patient	Sex	Weight (kg)	Age (days)	GA (weeks)
1	f	3.17	1	39
2	m	3.05	35	35
3	m	4.64	240	40
4	m	2.75	5	36
5	f	3.17	5	39
6	m	3.20	3	39
7	f	2.62	3	39
8	m	3.66	3	42

Patient	Main Diagnosis	Intubation (days)	PaO_2/FiO_2	Ventilator Mode
1	Surgery	1	305	HFOV
2	Encephalopathy	3	334	SIMV
3	ABCA3 mutation	240	140	SIPPV
4	Sepsis	5	298	SIMV
5	CDH	5	168	SIMV
6	CDH	3	325	SIMV
7	CDH	3	114	HFOV
8	CDH	3	197	HFOV + SIMV

Table 1. *Clinical characteristics of patients. Age*: age at the beginning of the study. *GA*: gestational age. Intubation: days of intubation before the beginning of the study. *PaO2/FiO2*: mean oxygen tension in arterial blood / inspiratory oxygen fraction. Ventilator Mode: HFOV = High Frequency Oscillatory Ventilation. SIMV = Synchronized Intermittent Mandatory Ventilation. SIPPV = Synchronized Intermittent Positive Pressure Ventilation. CDH = Congenital Diaphragmatic Hernia. ABCA3 = ATP-binding cassette sub-family A member 3.

Stable Isotopes Infusion Protocol

At time 0, all infants received a loading dose of 1 ml/kg body weight (BW) of 99% $^{2}H_2O$ (deuterium, Spectra 2000, Rome, Italy) followed by 0.0625% of fluid intake as $^{2}H_2O$ every 6 h over the next 48 h to maintain body water deuterium enrichment at plateau[106]. Tracheal aspirates (TA) were collected before tracer administration and every 6 h until 72 h and every 12 h until extubation or until day 5. TA collection method have been standardized and reported[107] and has been done as follows: 1 mL of 0.9% saline was instilled into the endotracheal tube, followed by collection of TA in a Lukens trap. Samples were kept at +4 °C and processed within 3 h. TAs were gently mixed and then centrifuged at 400 x g for 10 min to discard mucus and cells, and the supernatant was stored at -80 °C until analysis. TAs with visible blood were discarded.

If not specifically reported, all chemicals were bought from Sigma Aldrich (Sigma Aldrich Italia, Milan, Italy) and were of analytical grade or better. All solvent ratios are expressed as volume/volume ratio.

Total Phospholipids Content

Preliminary phosphorus assay[108] was performed on TA to assess total PL content to avoid column overload which would result in decreased recovery, lower selectivity, and carryover of PC in the PG fraction[109].

Liquid-Liquid Extraction

After adding 10 mg of phosphatidylcholine (PC) C-15 (Sigma Aldrich Italia) and 6 mg of PG C-15 (Avanti Polar Lipids, Alabaster, Alabama, USA) as internal standards (there is no endogenous production of odd fatty acids in humans), TA samples were mixed with 2 volumes of chloroform/methanol/hydrochloric acid 3/2/0.005N, vortexed for 10 minutes, centrifuged 10 minutes at 400 x g and the organic phase at the bottom of the tube was recovered. The procedure was repeated, and the recovered organic phases were combined.

Solid Phase Extraction of Phospholipids

The collected organic phases were evaporated to dryness at 37°C under a gentle nitrogen stream, re-dissolved in dichloromethane, and loaded onto 100 mg silica-NH2 columns (Bond Elute NH2, Variant Inc, Santa Clara, CA, USA) previously

activated with 1ml of n-hexane 4 times. Lipids were eluted under vacuum sequentially with: 1 ml dichlorometane/2-propanol (2/1); 1 ml glacial acetic acid/diethyl ether (2/98) and 2 ml of methanol. Subsequently the column was connected to a second pre-activated 100 mg silica-NH2 column and PG was eluted with 3 ml of dichloromethane/methanol/ammonium hydroxide (30%)/ammonium acetate (10 mM in methanol) (28/7/1/1).

HPTLC purification of PG

The PG fraction was dried under gentle nitrogen steam at 37°C, re-dissolved in 50 µl of chloroform/methanol (2/1), and spotted onto a 10x10 cm HPTLC plate (Nano-silica gel on TLC plates, Fluka, Buchs, Switzerland), previously impregnated (except for the spotting area) with boric acid 1.2% in water/ethanol (1/1) and activated for 1h at 100°C. After the spotting, the plate was developed with chloroform/ethanol/water/triethylamine (30/35/7/35). Developed HPTLC plates were nebulized with 2,7-dichlorofluorescein 0.2% in ethanol, and exposed to UV light at 254 nm to reveal the PG spot. PG identification was assessed by comparison with the retention factor (Rf) of lipid standards. PL's Rf were PG = 0.64 and PC = 0.15 (Figure 3) [110,111]. PG spots were finally scraped from the plates into Pyrex tubes for successive methylation.

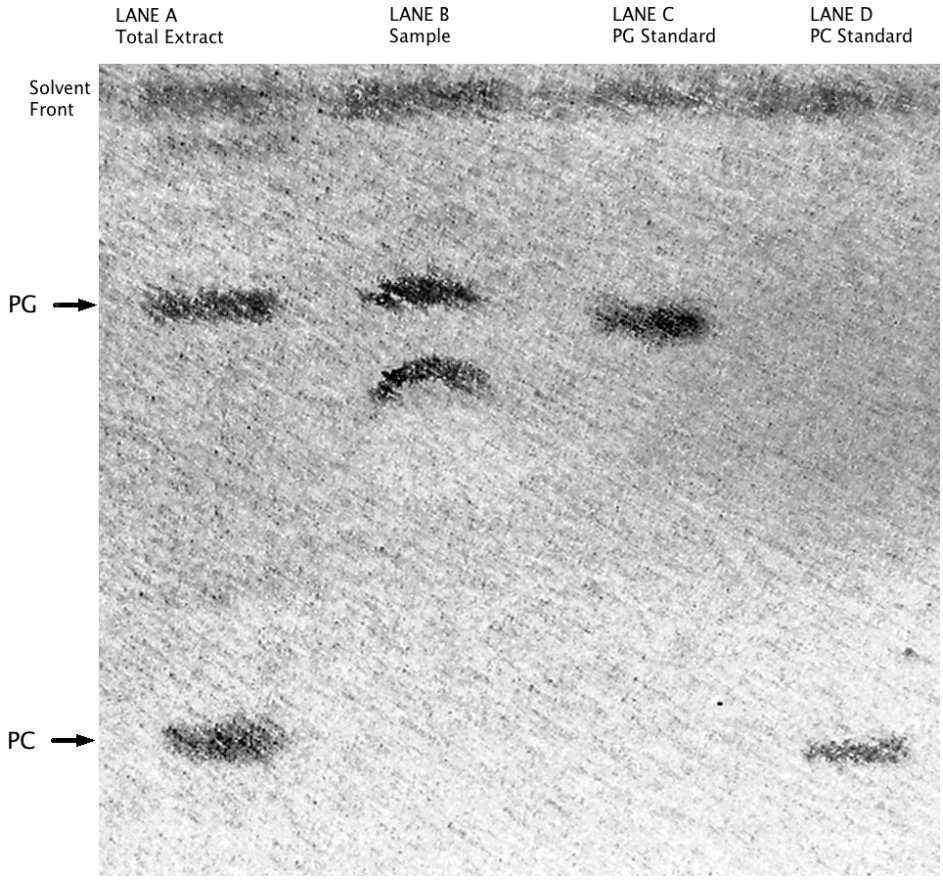

Figure 3. *HPTLC of different phases of PG isolation. Lane A*: total extract with no further purification. *Lane B*: purified PG fraction coming from column chromatography. *Lane C*: commercial PG standard. *Lane D*: commercial PC standard. Both standards were from frozen egg yolk (Sigma Aldrich Italia). The colors are inverted. The curved spot under the PG spot contains no PL and is not enriched. It is probably a manufacture plastic/oil residue.

TLC isolation of DSPC

The fraction eluted with methanol during solid phase chromatography was evaporated to dryness under nitrogen stream at 37°C, and DSPC was isolated from contaminating PLs with some modification of the procedure described by Mason *et al* [112]. The dried fraction was combined with 500 µl of 10mg/ml osmium tetroxyde in carbon tetrachloride, and left for 8 hours at room temperature in the dark. Samples were then dried under nitrogen, dissolved in 100 µl of chloroform/methanol (2/1), spotted onto 20x20 cm silica gel plates (Silicagel 60, Merck KGaA, Darmstadt, Germany) and developed with a solution of

choloform/methanol/isopropanol/triethylamine/potassium chloride 0.5% in water (40/12/33.3/24/8). The DSPC spot was identified with a commercial standard running in parallel with the samples[113], and then scraped into Pyrex tubes.

PG and DSPC fatty acids methyl ester preparation

To perform the GC/MS and GC-C-IRMS analysis, PG and DSPC fatty acids were hydrolyzed and derivatized by methylation (for fatty acid volatilization) under acidic conditions as follows[107,114,113]. Lipids fractions were evaporated under nitrogen stream and heated at 100°C for 1 h with 3 mL of methanolic HCl 3N (Sigma-Aldrich). The solutions were then cooled and neutralized with a solution of $CaCO_3$ 10%. Two-hundred µl of n-hexane + 50 mg/L of butylated hydroxytoluene (BHT) were added to the neutralized solution, mixed for 10 minutes and centrifuged at 400 x g for 10 minutes. The upper n-hexane phase, containing esterified fatty acids was transferred to a glass vial-insert and analyzed[106,113].

Quantification of PG and DSPC

Fatty acid methyl esters were injected into a GC-FID system (HP 5890, Palo Alto, CA, USA) and their amounts were determined[115] comparing fatty acid peaks areas using the previously added C-15 fatty acid as internal standard[114].

Contamination of PG by DSPC

Separation of PG from other lipid classes on the HPTLC plate is shown in Figure 3. Since PG kinetics is derived from palmitate deuterium enrichment and palmitate is also the main fatty acid in DSPC, it was mandatory to demonstrate no contamination of PG by DSPC. To this end, we extracted phospholipids of 2 TA samples to combine 100 µg of PLs of each TA with 0.5 µg of U-^{13}C-palmitate DPPC (Avanti Polar Lipids). ^{13}C-palmitate contamination was estimated by single quadrupole GC-MS (Voyager, Thermoquest, Rodano, Milan, Italy) operating in chemical negative ionization mode. The experiment was done in triplicate and results were expressed as tracer to tracee ratio (TTR)[87,107,116-118].

Measurement of deuterium enrichment

Palmitate-DSPC (DSPC-PA) and palmitate- PG (PG-PA) methyl ester deuterium enrichments were measured by GC-C-IRMS (DELTA plus XL, Thermo Electron

Corporation, Rodano, Italy). The DSPC and PG fatty acids were separated in a GC (HP 6890, Palo Alto, CA, USA) equipped with a fused-silica column (Ultra 2, 25 m × 0.25 mm internal diameter, 0.25-µm film thickness; J&W Scientific Agilent Technologies Italia S.P.A, Cernusco sul Naviglio, Milano, Italy)[106] and the $^{2}H/^{1}H$ ratios of the hydrogen gas obtained by quantitative pyrolysis (1400°C) were determined by the simultaneous integration of the *m*/*z* 2 ($^{1}H^{1}H$) and *m*/*z* 3 ($^{2}H^{1}H$) ion beams over time. The $^{2}H/^{1}H$ ratios were automatically corrected by the ISODAT 2.0 software for the H^{3+} contribution to *m*/*z* 3, the chemical background, and the isotopic time shift on the GC column. Each sample was analyzed in triplicate. A blank run with pure n-hexane was interspersed every six injections to insure absence of palmitate ghost peaks and avoid memory effect.

Urine deuterium enrichment

Urinary deuterium enrichment, representative of the body water enrichment, was measured by a thermal conversion/elemental analysis (TC/EA, Thermo Electron Corporation) device coupled with an IRMS. One hundred µl of urine were deproteinized with sulphosalicylic acid, cooled in an ice bath for 10 minutes and centrifuged at 2300 x g for 10 minutes. The supernatant was isolated, diluted 1/20 (except for the initial sample) with distilled water of known isotopic enrichment and injected into the TC/EA device[119].

Calculations and kinetic analysis

Results were expressed as ð (delta) $^{2}H[‰]$ = (1000 ð x ($^{2}H/^{1}H$sample - $^{2}H/^{1}H$standard)/$^{2}H/^{1}H$standard). The δ ^{2}H represents the increase in isotopic enrichment above baseline of ^{2}H. Urine enrichments were normalized against Vienna Standard Mean Ocean Water (VSMOW, International Atomic Energy Agency, Vienna, Austria), which defines 0‰ as δ ^{2}H. Delta ^{2}H values of fatty acids vs. VSMOW were obtained using a standard mixture of fatty acids with standard δ ^{2}H ("Mixture F8", kindly provided by Prof. Arndt Schimmelmann, Dept. of Geological Sciences, University of Indiana, Bloomington, IN, USA)[120].

The fractional synthesis rate (FSR) was obtained by dividing the slope of the linear enrichment increase of TA palmitate-DSPC and palmitate-PG by the urine enrichments multiplied by 64.8%, that represents the maximum quantity of deuterium that could be incorporated during the synthesis of palmitate[121].

DSPC and PG FSRs were calculated using to the same time range and with urine deuterium enrichments at steady state.

Peak time (PT) was the time required to reach maximum enrichment of palmitate-DSPC and PG.

Secretion Time (ST) was the time of intersection between the slope of the linear increase of palmitate-DSPC and PG enrichments and the X axis.

Clinical and kinetics data are expressed as mean ± standard deviation, or as median [first quartile – third quartile] as appropriate.

Comparisons were done with Wilcoxon t-test and differences were considered significant if $p < 0.05$. Correlations were assessed by Pearson "r" test. Analysis was performed using Microsoft Excel 2003 (Microsoft Corp. Redmon, WA, USA) and Prism 4.0 (GraphPad Software Inc. La Jolla, CA, USA).

RESULTS

Patients

No side effects were observed after the administration of $^{2}H_2O$. Patient clinical characteristics are reported in Table 1. Two infants had no lung disease and needed mechanical ventilation one for abdominal surgery and one for neurologic failure. Four had congenital diaphragmatic hernia (CDH), one was heterozygote for the ATP-binding cassette sub-family A member 3 (ABCA3) mutation and one had sepsis. PaO_2/FiO_2 ratio ranged from 114 to 334 (Table 2).

Patient	δ Urine (^{2}H ‰)	ST_{DSPC} (hours)	PT_{DSPC} (hours)	FSR_{DSPC} (%/day)	ST_{PG} (hours)	PT_{PG} (hours)	FSR_{PG} (%/day)
1	8510.51	0.2	71	6.48	0.4	30	5.84
2	7331.89	15.1	97	6.56	25.0	54	3.58
3	2992.67	14.5	42	14.97	24.6	36	33.58
4	7018.57	3.7	30	15.09	3.9	26	13.18
5	7024.48	0.1	73.5	4.46	21.1	68.5	5.04
6	7842.44	1.6	105	7.27	19.3	51	8.67
7	7722.62	12.4	62.5	6.05	8.9	49	4.67
8	7372.69	8.8	66	8.71	12.4	41.5	10.62
Median Interquartile Range]	7331.9 [7018.6 – 7722.6]	3.7 [0.9 -13.4]	71.0 [52.2 – 85.2]	6.6 [6.3 – 11.1]	19.3 [6.4 – 22.8]	49.0 [33.0-52.5]	5.8 [4.8 – 10.9]

Table 2. *Kinetics data. δ Urine*: urinary deuterium enrichment expresses as δ ^{2}H ‰. *ST*: secretion time. *PT:* peak time. *FSR*: fractional synthetic rate. See text for detailed description of abbreviations.

PG Purity

The TTR of ^{13}C palmitate-DSPC and ^{13}C palmitate-PG aliquots with no addition of U-^{13}C-DPPC were 0.0002 ± 0.0001 and 0.0018 ± 0.01 respectively. TTRs of palmitate-DSPC and palmitate-PG in the aliquots where U-^{13}C-DPPC was added were respectively 0.10 ± 0.01 and 0.0016 ± 0.01. Thus ^{13}C palmitate-DPPC contamination in PG fraction was estimated to be 0.8%. The analysis was confirmed by GC-C-IRMS.

Kinetic data

Palmitate-DSPC and PG kinetics were successfully measured in all patients. All infants achieved body water isotopic deuterium enrichment plateau (inferred from urine enrichment) within 6 h from the start of the study. Isotopic equilibrium was maintained over the next 48 h by administering ^2H_2O. Mean urine deuterium enrichment at equilibrium was 7331.9 [7018.6 – 7722.6] ‰. In the patient 3, urinary enrichment plateau was 2993.7 ‰, due to the administration of a lower dose of deuterated water. Figure 4 shows a typical pattern of deuterium enrichment in DSPC-palmitate of and PG-palmitate isolated from tracheal aspirates. As shown in Table 2, median ST, PT, and FSR for DSPC were respectively: 3.7 [0.9 – 13.4] h, 71.0 [52.2 – 85.2] h and 6.6 [6.3 – 11.1] %/day. Median ST, PT and FSR for PG were respectively: 19.3 [6.4 – 22.8] h, 49.0 [33.0 – 52.5] h and 5.8 [4.8 – 10.9] %/day. The peak time (PT) of PG was significantly shorter than that of DSPC ($p<0.01$). Figure 3 shows that the FSR of DSPC was significantly correlated with that of PG ($R^2 = 0.6597$, $P = 0.01$).

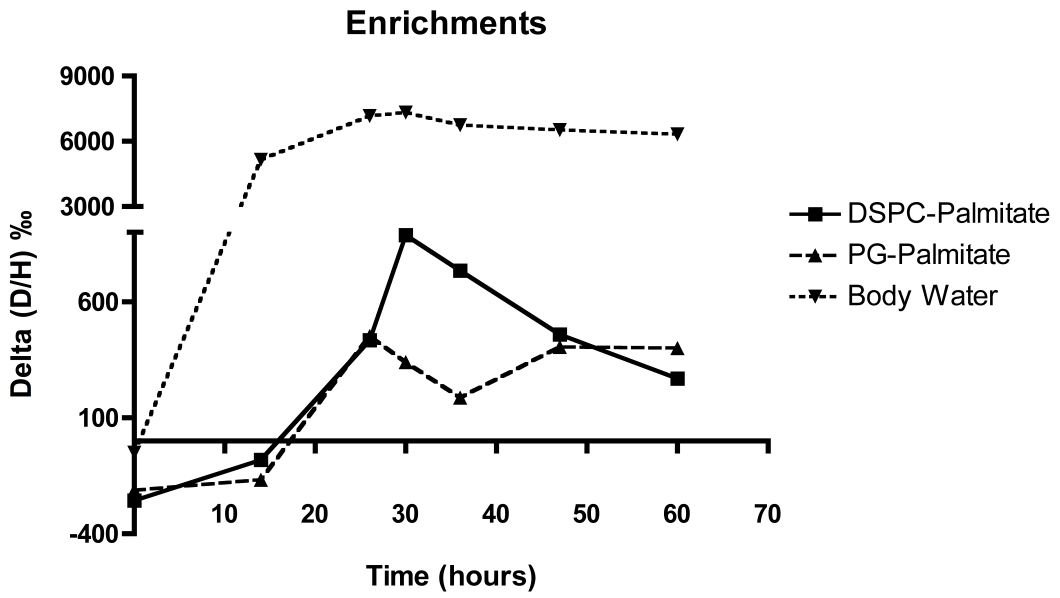

Figure 4. *Enrichment curves of PG and DSPC palmitate residues in one study infant.* The figure shows an example of the enrichment patterns of PG and DSPC palmitate residues. The DSPC pattern reaches a peak after 30 hours from the beginning of the study, and then slowly falls. On the other hand, the PG pattern is irregular probably due to a more complex degradation pattern than DSPC. The line on the top shows the enrichment pattern of the body water of the patient.

DSPC and PG in TAs

DSPC and PG founded in TAs, expressed as % of total PL, were: 49.5 [44.1 – 50.7]% for DSPC and 12.5 [10.3 – 13.8] % for PG. The overall recovery calculated using a C-15 internal standard for each PL was 50 ± 10% for PG and 90 ± 12% for DSPC. DSPC and PG fatty acid compositions are reported in Table 3.

PL-FA	PG %	DSPC %
C12:0	4.6 ± 3.6	
C14:0	3.8 ± 1.3	9.1 ± 1.9
C16:0	37.3 ± 4.8	86.4 ± 2.1
C16:1ω7	1.8 ± 1.4	
C16:1ω9	3.9 ± 1.9	
C18:0	17.3 ± 6.9	4.5 ± 1.8
C18:1ω9	20.1 ± 5.3	
C18:2ω6	4.2 ± 1.5	
C18:3ω6	5.5 ± 3.6	
C18:3ω3	1.5 ± 1.1	
C16:1ω9	1.4 ± 0.9	
C20:4ω6	2.4 ± 1.0	

Table 3. *Fatty Acid composition of PG and DSPC.* Results as % (mean ± SD) of total fatty acids (FA). Results are calculated by averaging the fatty acid composition of all time points of all study infants.

DISCUSSION

In this study we simultaneously analyzed airway DSPC and PG kinetics in newborn infants. We show for the first time that DSPC and PG kinetics can be measured *in vivo* in infants with and without pulmonary disease, with no modification of the clinical routine.

The lungs are the only mammalian tissue containing significant amounts of PG, which is synthesized in the endoplasmic reticulum and thereafter is transferred via the Golgi system to the lamellar bodies, from where it enters the alveolar spaces together with other surfactant components. PL synthesis in alveolar type II cells does not differ significantly from other cell types and tissues except for

the peculiar property of producing preferentially disaturated and monoenoic phosphatidylcholines (PCs) [17]. DSPC and PG relative concentration and fatty acid composition presented in this study (Table 3) are in agreement with previous studies in humans[99,122,123].

The incorporation of tracers into lung DSPC has been extensively used as a way to study surfactant turnover, however, there is evidence that individual surfactant components may turn over at different rates, implying a more complex picture of the surfactant life-cycle[105]. We found that ST, PT and FSR assumed a rather wide spectrum of values, possibly due to the heterogeneity of clinical conditions. There was however, a significant correlation (Figure 5) between the fractional synthetic rates of palmitate-PG and -DSPC, suggesting that the overall turnover rates of these two phospholipids are closely related. This conclusion is in agreement with the results of animal studies[124,125] and with the fact that DSPC, PG and phosphatidyl-inositol (PI) originate from interconnected synthetic pathways[17]. Indeed, in type II pneumocytes isolated from rabbits at late gestation [21,23,126] an increase in DSPC synthesis is accompanied by an increase in PG synthesis and a decrease in PI synthesis [23].

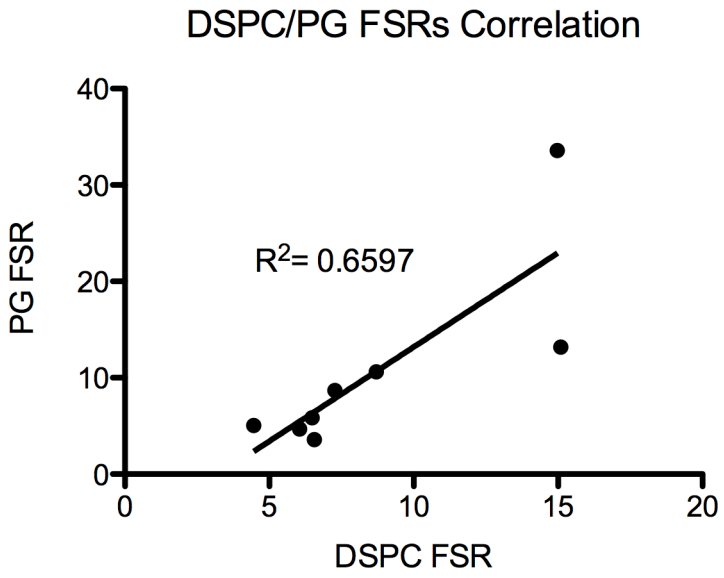

Figure 5. *Correlation between the fractional synthesis rate (FSR) of DSPC and PG.* Pearson's r test: r = 0.8122, P = 0.01. FSR is the percentage of each PL synthesized in 24h.

The time to maximum incorporation of tracer was significantly shorter for PG with respect to DSPC (Table 2). Considering that the fractional synthetic rate of DSPC was similar to that of PG and that patients appeared to be at steady state (as suggested by a constant recovery of DSPC from TAs), we interpret the shorter PT of PG as an indication that PG may cycle between type II cells and the alveoli at a faster rate that DSPG, while the overall rate of removal of the two phospholipids from the surfactant system is similar. In cell and animal studies PG appears to be involved in a regulated, specific degradation pattern that involves macrophages. Notable is the fact by which PG is preferentially internalized by macrophages when SP-A is not present. When SP-A is added, lipids uptake is enhanced for both PG and DPPC, as occurs when macrophages are attached to plastic and not in suspension. Moreover phospholipases from macrophages homogenate showed a preferential activity toward PG than DPPC[104,105]. Finally, recent studies added more complexity to this scenario, underlining that PG is not only implicated in lowering superficial tension in alveoli but it actively interacts with inflammatory cells by modulating their responses to various inflammatory stimuli[127-129]. These *in vitro* data are consistent with our finding that PG metabolism is regulated in a different pathway than DSPC.

From the present data only DSPC half-life could be calculated using the descending part of the enrichment curve [87 125], since the decay curve of PG is not linear (Figure 4).

A methodological limit of this study concerns primarily the TLC step that prolongs analytical time.

Stable isotopes coupled with the sensitivity of GC-C-IRMS can be a valid technique to study the turnover of various surfactant components. Due to the sensitivity of the instrumentation, the analysis requires a high purity of the components under investigation. To achieve this goal, HPLC and UPLC techniques could be successfully employed prior to IRMS measurements[130]. Alternatively, a more simple (in terms of instrumentation needed) purification using TLC as a fundamental step could successfully be utilized to achieve comparable results in terms of purity with an initial concentration in the range of a few nanomoles of analytes[109].

In summary, we show that it is feasible to simultaneously measure palmitate DSPC and PG kinetics in infants using deuterated water as metabolic precursor

of palmitate. PG is metabolized and probably produced in pathways differently regulated from the DSPC ones. The study of the individual faiths of surfactant components is crucial to unveil the mechanisms that lead to surfactant inactivation and thus to the severity of life-threatening diseases like RDS and ARDS.

This study was published as:

Vedovelli L, Baritussio A, Carnielli VP, Simonato M, Giusti P, Cogo PE. Simultaneous measurement of phosphatidylglycerol and disaturated-phosphatidylcholine palmitate kinetics from alveolar surfactant. Study in infants with stable isotope tracer, coupled with isotope ratio mass spectrometry. *J Mass Spectrom.* Oct 2011;46(10):986-992.

Chapter Four

Protein Metabolism: Disaturated Phosphatidylcholine and Specific Protein B

BACKGROUND

Acute (formerly "adult") Respiratory Distress Syndrome (ARDS) is characterized by bilateral radiographic infiltrates and a ratio of the partial pressure of arterial oxygen to the fraction of inspired oxygen (PaO_2/FiO_2) < 200. Acute Lung Injury (ALI) is a less severe form of respiratory distress with a PaO_2/FiO_2 between 200 and 300 [76]. In both clinical entities reduced lung compliance and surfactant inactivation contributes to respiratory failure [80,99,131]. Proposed mechanisms of lung injury include destruction of the air-water interface by alveolar oedema, phospholipids degradation by secretory phospholipases, degradation of surfactant proteins by proteases [132,133], damage by reactive oxygen species and decreased synthesis of surfactant components by damaged type II cells [134]. Moreover, leakage of plasma proteins into the alveoli is thought to decrease alveolar stability [135]. *In vitro*, non-surfactant specific proteins (i.e. blood and plasma proteins) have been shown to compete with the lipids for adsorption at the air water interface, leading to the formation of an interfacial film less prone to incorporate surfactant phospholipids [136].

Pulmonary surfactant is composed by 90% lipids, mostly phospholipids, and 10% of specific proteins [97]. Surfactant Protein B (SP-B) is a small hydrophobic protein synthesized as a pre-protein (pro-SP-B) and processed to mature form *en route* from the Golgi complex to the lamellar bodies [137]. Mature SP-B is secreted as a surfactant component into the alveolar space where it is mainly found as a dimer [138]. Clara cells also express pro-SP-B, but they do not process the protein to the mature form [139]. SP-B enhances the rate of phospholipids adsorption to the alveolar air/water interface [140], decreases surface tension by interfering with

the attractive forces acting between water molecules [141] and has anti-inflammatory properties [80,99].

Clinical studies have shown that disaturated phosphatidylcholine (DSPC) is markedly decreased in bronchoalveolar lavage fluid of adult ARDS patients, whereas the phosphatidylcholine content is only slightly decreased [80,99]. SP-B has also been reported to be reduced by 25-55% in tracheal aspirates of adult ARDS/ALI patients [80,133] but in association with normal levels of SP-B mRNA [142]. Conversely a recent study performed in children confirmed a significant decrease of DSPC but no significant changes in SP-B levels in bronchoalveolar lavage fluid of ALI/ARDS children compared with controls[143]. Decreased levels of DSPC and SP-B could be due to increased degradation, decreased synthesis or both. The goal of this investigation was to measure the rate of synthesis of DSPC and SP-B in ARDS/ALI patients and in controls with normal lungs.

METHODS

Patients were studied from 2003 to 2006. ARDS and ALI cases were defined by the AECC criteria [76]. Twelve patients were recruited within 72 hours from the onset of the respiratory failure. Causes of ARDS/ALI were pneumonia in 6 patients, poly-trauma in 4, pancreatitis in 1 and aspiration of gastric contents in 1. Eight patients without lung disease, who needed mechanical ventilation after major surgery or for neurological failure, were enrolled as controls. Exclusion criteria were: presence of liver failure, defined as transaminases (GOT, GPT) > 3 times normal values, renal failure (creatinine > 2 times normal values), burns > 30% body surface area, bone marrow or lung transplantation. The local ethical committee approved the study, and informed consent was obtained for all the patients.

Clinical data, ventilator parameters, arterial blood gas analysis and transcutaneous saturation were recorded at the start of the study and then every 6 hours during the study period. Routine blood tests performed at the admission to the Intensive Care Unit and during the study according to the standard unit practice were also recorded in order to detect signs of nosocomial infection or of organ failure. For each patient SAPS II score (Simplified Acute

Physiology Score, that describes the severity of a disease) was calculated at study entry.

Study design

All patients received a constant intravenous infusion of 1 g 1-^{13}C Leucine (Cambridge Isotope Laboratories, Andover, MA) dissolved in water for injection for 24 h. Deuterated water $^{2}H_2O$ (Cambridge Isotope Laboratories) was administered as a 25 ml bolus at the study start and then, every 12 hours over the next 36 hours, as intermittent boluses corresponding to 0.0625% of fluid intake, to maintain steady state of deuterium enrichment in body water [106].

Blood (0.6 ml), urine (1 ml) and tracheal aspirates [85] were collected at times 0, 6, 12, 18, 24, 30, 36, 42, 48 hours and then every 12 hours until extubation. Tracheal aspirates and blood samples were centrifuged at 400 x g and 1300x g respectively and supernatants were stored at -80°C.

Tracheal aspirates' protein and phospholipids analysis

Total proteins from tracheal aspirates were determined at time 0 or within the first 24 hours [144]. Phospholipids phosphorous was measured in tracheal aspirate samples from the study start until 48 hours [108].

DSPC was extracted and separated from tracheal aspirates according to standard methods [145] and DSPC fatty acids derivatized as methyl-esters and measured by gas chromatography (see Chapter Three for details) [85].

SP-B amounts were quantified by ELISA on non-fractionated tracheal aspirates obtained at the beginning of the study or within 24 hours [146] using a rabbit antiserum directed against mature SP-B [147].

DSPC, SP-B and protein concentrations in aspirates, were normalized to alveolar lining fluid using the urea method (BioAssay Systems, Hayward, CA)[148].

Isolation of SP-B from tracheal aspirates

SP-B was isolated from tracheal aspirates and hydrolyzed as follows: SP-B was isolated from lipid extract with Bond Elute NH_2 containing 100 mg resin (Supelco, Milano, Italy) preconditioned with 3-5 ml of chloroform. After loading the sample, the columns were eluted sequentially with 3 ml of the following chloroform/methanol/acetic acid mixtures: 20:1:0; 9:1:0; 4:1:0; 4:1:0.025; 3:2:0;

1:4:0; 1:9:0. SP-B fraction (4:1:0 and 4:1:0.025) were pooled together, dried under nitrogen stream and hydrolysed to free amino acids by 0.5 ml of HCl 6 N for 24 h at 110°C. Individual amino acids were derivatized into their N-acetyl-n-propyl derivatives[149] and the ^{13}C enrichment of leucine measured by mass spectrometry (GC-MS Voyager, Thermoquest, Milan, Italy) [150].

Plasma leucine enrichment

One hundred µl of plasma were deproteinized with sulphosalicilic acid (6% w/v) and plasma amino acids were derivatized as N(O,S)ethoxycarbonyl esters in a aqueous solution of ethyl chloroformate [151]. Free plasma leucine enrichment was measured by gas chromatography mass spectrometry (GC/MS). Results were expressed as Mole Percent Excess with reference to a calibration curve for 1-^{13}C Leucine.

Urine deuterium enrichment

One hundred µl of urine were deproteinized with sulphosalicilic acid (6% w/v) and diluted 1:10 with local distilled reference water. Urine deuterium enrichment was analysed by a High Temperature Conversion Elemental Analyser coupled with an Isotope Ratio-Mass Spectrometer (TC-EA-IRMS, Thermo Scientific, Bremen, Germany) [119]. Enrichment was expressed as delta ‰.

The ^{2}H enrichment of DSPC-palmitate was analyzed by GC-C-IRMS and expressed in delta ‰ after correction for isotopic contribution of the derivative group[106].

Calculations

All kinetic measurements were performed assuming a steady state. The assumption was based on the following considerations: 1) in all patients plasma 1^{13}C leucine and urine $^{2}H_2O$ enrichments reached steady state within 6 h from the start of the isotope infusion; 2) the slope of the enrichment curve over time did not deviate significantly from zero between time 6 h and time 24 h for plasma leucine and between time 6 h and time 36 h for urine $^{2}H_2O$; 3) the concentrations of DSPC and SP-B in tracheal aspirates did not change significantly during the first 48 hours of the study.

Tissue-bound and alveolar surfactant was regarded as one pool. The fractional synthesis rate (FSR) was calculated as describe in Chapter Three [85,106].

Clinical and kinetic variables were expressed as mean±SD or median (interquartile range) as appropriate. Statistical analysis was performed by a non-parametric test (Mann-Whitney test). Significance was defined as $p<0.05$. Data were analysed using the statistical package SPSS 15 (SPSS Inc, Chicago, IL).

RESULTS

Clinical characteristics

Twelve ARDS/ALI and 8 control adults were studied. Clinical characteristics and ventilator parameters are reported in Table 1. Only 4 of the 8 controls were on mechanical ventilation, the remaining patients were on spontaneous breathing through a tracheostomy. All ARDS/ALI patients exhibited severe derangement of gas exchange at the time of the study start (which corresponded to the first tracheal aspirate collection) with a PaO_2/FiO_2 ratio of 185 ± 61. Thereafter PaO_2/FiO_2 values progressively improved, but remained markedly lower than control values (Table 1). Two of the 20 patients (both with ARDS) died within 30 days from the study start.

	Patients		p value
	ARDS/ALI (N=11)	CONTROLS (N=8)	
Male/Female (n°)	6/5	4/4	
Age (y)	53 ± 16	48 ± 24	0.66
Body weight (Kg)	80 ± 16	69 ± 19	0.21
Survival Rate	82%	100%	
SAPS II	37 ± 12	37 ± 5	0.46
PIP at the start of the study (cm H_2O)	25 ± 6	14 ± 4 (4/8)	<0.01
PIP during the study (cm H_2O)	24 ± 6	14 ± 4 (4/8)	0.05
PEEP at the start of the study (cm H_2O)	9 ± 2	3 ± 1 (4/8)	<0.01
PEEP during the study (cm H_2O)	9 ± 2	3 ± 0.4 (4/8)	<0.01
PaO_2/FiO_2 at the start of the study	185 ± 61	365 ± 72	<0.001
PaO_2/FiO_2 during the study period	208 ± 46	383 ± 82	<0.001
$AaDO_2$ at the start of the study (mmHg)	309 ± 111	71 ± 27	<0.001
$AaDO_2$ during the study (mmHg)	255 ± 84	74 ± 41	<0.001
Tidal Volume (ml/Kg bw)	7 ± 1	7 ± 1 (4/8)	0.54

Table 1. *Clinical characteristics and ventilatory parameters of study patients.* Mean ± SD. PaO_2/FiO_2 = mean oxygen tension in arterial blood/inspiratory oxygen fraction. PEEP = positive end expiratory pressure. PIP = peak inspiratory pressure. $AaDO_2$ = Alveolar arterial oxygen gradient. SAPS II = scores on the acute physiology and chronic health evaluation. Values compared with Mann-Whitney test.

Surfactant composition

Total proteins, total phospholipids, DSPC, and SP-B concentrations, normalized to epithelial lining fluid, at study start are shown in Table 2. In patients with ARDS/ALI total protein concentration were higher, ($p<0.05$), total phospholipids were not different, and DSPC and SP-B were markedly and significantly lower than in controls. DSPC and SP-B concentrations were 16.9% and 40.5% of the control values respectively.

DSPC, as percentage of total phospholipids, was lower in ARDS/ALI than in controls throughout the study ($p<0.01$).

	Patients		p value
	ARDS/ALI (N=11)	CONTROLS (N=8)	
Total phospholipids (mg/ml ELF)	0.98 (0.57-1.30)	2.30 (1.03-1.66)	0.07
Total protein (mg/ml ELF)	68.6 (46.3-97.2)	44.7 (33.7-49.1)	<0.05
PPQ	0.010 (0.014-0.036)	0.034 (0.024-0.051)	<0.01
SP-B (µg/ml ELF)	1.7 (0.8-2.9)	4.2 (3.4-5.8)	<0.05
SP-B (%PL)	0.21 (0.08-0.36)	0.21 (0.11-0.44)	0.7
DSPC (mg/ml ELF)	0.11 (0.08-0.24)	0.65 (0.50-2.59)	<0.01
Mean DSPC (%PL)	50 (43-51)	54 (52-58)	<0.01

Table 2. *Surfactant composition of tracheal aspirates* All data represent as median and interquartile range. PPQ = Phospholipids-to-Protein quotient. ELF= epithelial lining fluid. Total protein, total phospholipids, DSPC and SP-B were determined in one tracheal aspirates at the start of the study or within 24h. Values were corrected for dilution using the urea method. DSPC (%PL) was determined in all tracheal aspirates collected till the end of the study. Values were compared using Mann-Whitney test.

Surfactant DSPC and SP-B kinetics

DSPC concentration in tracheal aspirates was measured every 6 hours for the first 48 hours in all ARDS/ALI patients to assess the steady state of the surfactant pool. Except for 1 ARDS patient, who was excluded from the study for an increasing DSPC concentration over time, all patients had DSPC concentration within 10% of coefficient of variation (data not shown), suggesting a steady state condition during the time frame of kinetics measurement. Enrichment curves of DSPC-palmitate and SP-B-leucine from ARDS patients and control subjects are shown in Figure 1. In most subjects SP-B enrichments returned to baseline within 60 hours from the start of the tracer infusion, while DSPC enrichments took about 150-200 hours to return to baseline.

SP-B turned over at a much faster rate than DSPC both in controls and in patients with ARDS/ALI (Figure 1). In controls SP-B turned over at a rate 28 times faster than DSPC.

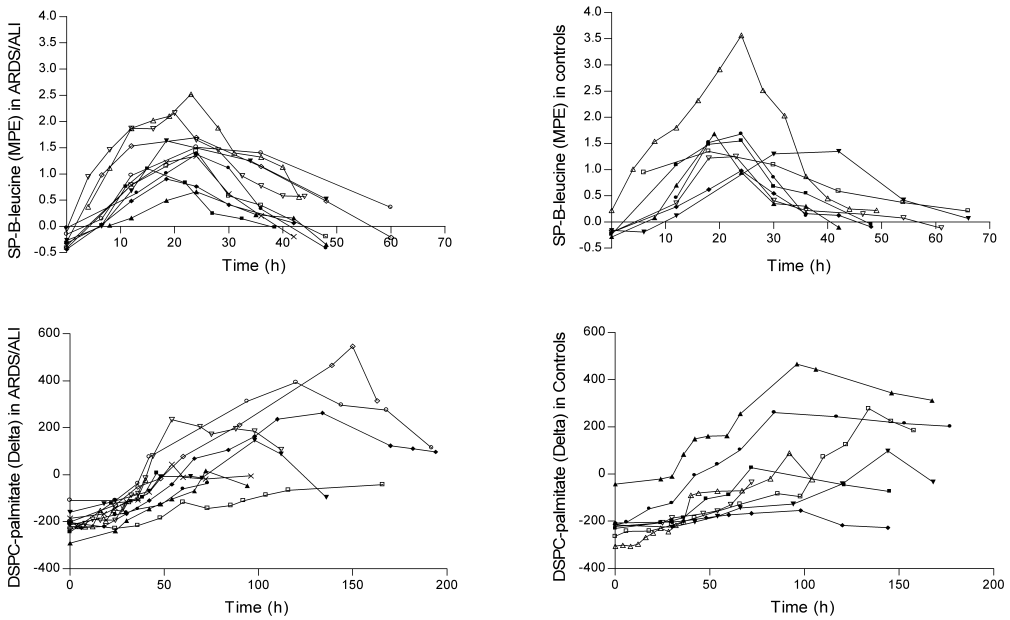

Figure 1. *SP-B leucine and DSPC-palmitate enrichment curves in ARDS/ALI and in control patients.* The ^{13}C-leucine (top panels) and deuterium-palmitate (bottom panels) enrichment curves of SP-B and DSPC obtained from tracheal aspirates. Each symbol represents a different subject. MPE: mole percent excess; Delta (^{2}H/^{1}H vs. VSMOW).

In ALI/ARDS the fractional synthesis rate of DSPC was 3.1 times higher than in controls ($p<0.01$), while the fractional synthesis rate of SP-B was not statistically different than in control subjects (Figure 2).

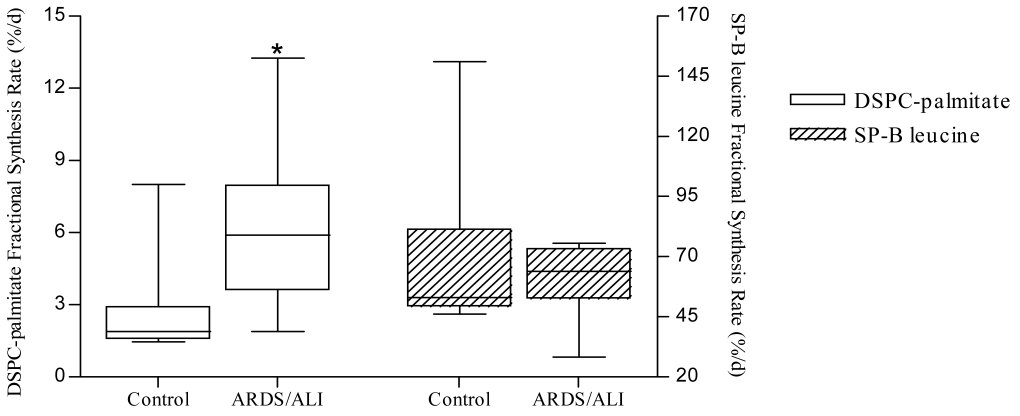

Figure 2. *Fractional synthetic rate of DSPC-palmitate and SP-B-leucine in ARDS/ALI and control patients.* Synthesis of DSPC-palmitate results to be significantly higher in ARDS/ALI group. SP-B-leucine synthesis is similar in the two groups. Results are expressed as median and interquartile ranges. * Significantly different from controls ($p<0.01$ by Mann-Whitney test).

DISCUSSION

In this study we provide novel information on the turnover of DSPC and SP-B in normal subjects and in patients with ARDS/ALI, while confirming that patients with ARDS/ALI have decreased levels of DSPC and SP-B and increased protein concentration in tracheal aspirates [80,131-133,142,152,153].

In agreement with previous animal studies [147,154], we found that SP-B is turned over at a faster rate than DSPC both in controls and in ARDS/ALI. Since SP-B and DSPC are packaged into lamellar bodies and then are secreted together, their different turnover rate could be explained by partitioning into distinctive alveolar structures (i.e. DSPC could distribute preferentially to the interfacial film or stay there for a longer time), by an intrinsically faster turnover of SP-B in the alveolar space or by the use of different pathways of recycling before packaging into lamellar body membranes. Human studies do not allow to further discriminate among these possibilities, since lung tissue could not be sampled. From animal experiments, though, we can extrapolate that all these mechanisms could be at play [147,154].

ARDS/ALI patients showed an increased synthesis rate of DSPC but not of SP-B. If the increased synthesis rate of DSPC seems a logical compensatory mechanism to increased phospholipids degradation or monolayer inactivation in

the injured lungs, the finding that in ARDS/ALI the rate of synthesis of SP-B is comparable to control subjects, was unexpected. Possible explanations are that ARDS/ALI patients cannot mount a compensatory enhanced synthesis of SP-B or, conversely, that the decrease of airway SP-B in our ARDS patients was not big enough to elicit the homeostatic response. In agreement with the last interpretation, a recent study with a transgenic mouse model expressing human TNF-alpha in respiratory epithelial cells showed that, after a 36-61% decrease of airway SP-B, the level of SP-B mRNA in lung tissue remained unchanged [142].

In the other hand, the lung appeared to "sense" the larger decrease in airway DSPC content and increased three fold its fractional rate of synthesis. The mechanism underlying this response remains unclear. A recent publication investigating the role of signal transducer and activator of transcription-3 (STAT-3, which is activated by members of IL-6-like group of pro-inflammatory cytokines [155]) found that in mice treated with LPS, the synthesis of DSPC and SP-B increased in a STAT-3 dependent way [156].

In this study we measured also DSPC and SP-B concentration in epithelial lining fluid as a proxy of surfactant pool. The estimation of airway surfactant pool by the measurement of individual surfactant components obtained from tracheal aspirates has limitations, since the recovery may vary, in spite of the standardization of the suction technique and the correction for dilution. Therefore the low concentrations of DSPC and SP-B recovered from tracheal aspirates of patients with ARDS/ALI could be due either to decreased surfactant concentration in the airways, or to the fact that collapsed areas may be less prone to release surfactant recoverable by aspiration or even to the sampling technique that could be affected by clinical severity. These observations can partially explain the controversial results reported on surfactant SP-B amount during ARDS/ALI [80,133,143].

Kinetic data obtained from tracer studies have the advantage of being independent from recovery. Tracer studies were classically performed in animals using radioactive tracers, and they showed that surfactant specific proteins A, B and C were turned over faster than DSPC [147,154]. We previously showed by administering DSPC labelled with stable isotopes through the airways, that in a population of patients with ARDS the airway DSPC pool was 10 fold smaller than in controls [87].

A further limit on the estimation of the airway surfactant composition and pool by tracheal aspirates derives from the fact that the currently available ELISA methods to measure SP-B cannot distinguish between the mature protein and its pro-forms, nor do they recognize modified SP-B, like oxidized SP-B, whose possible pathogenetic role has been recently underlined [157]. Here we separated mature SP-B by sorbent chromatography and thus provides kinetic data regarding solely mature SP-B.

Since the concentrations of DSPC and SP-B in the tracheal aspirates of patients with ARDS/ALI did not change significantly during the sampling period, we assumed that patients were at steady state, with synthesis matching degradation for both surfactant components. However, due to the uncertainty about the true dimensions of the alveolar pool of DSPC and SP-B, the present data did not allow us to calculate the absolute rate of synthesis of these compounds [91].

In conclusion, our results can be summarized as follows: 1) DSPC and SP-B turned over with different kinetics in the airways both in human adults with normal lungs and in patients with ARDS/ALI, 2) in patients with ARDS/ALI in spite of the low concentration of DSPC and SP-B in tracheal aspirates, the fractional synthesis rate of DSPC increased, while that of SP-B did not change significantly.

This study was published as:

Simonato M, Baritussio A, Ori C, Vedovelli L, Rossi S, Dalla Massara L, et al. Disaturated-phosphatidylcholine and surfactant protein-B turnover in human acute lung injury and in control patients. *Respir Res*. 2011;12:36.

Chapter Five

Preliminary Study on the Role of H^+ V-ATPase Proton Pump

BACKGROUND

Before secretion, alveolar Type II cells store and process alveolar surfactant to the mature form into lysosome-like organelles called lamellar bodies (Figure 1).

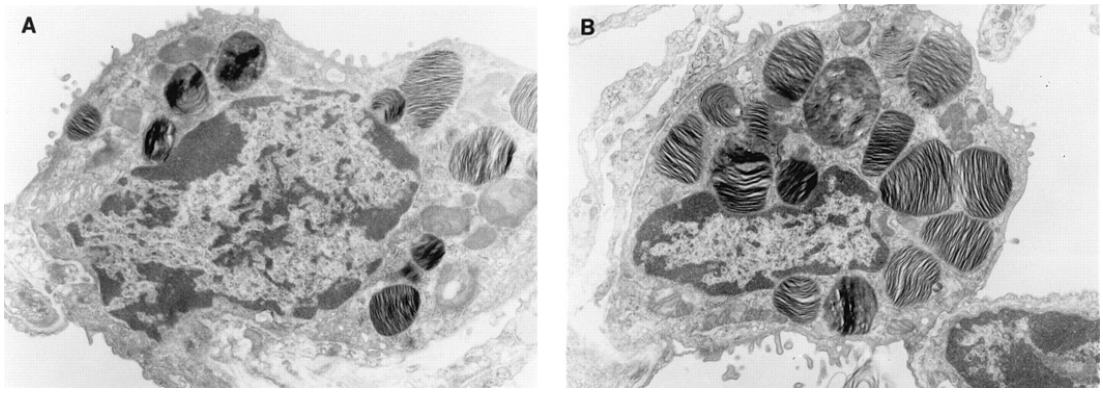

Figure 1. *Electron microscope image of a Type II cell.* Lung tissue from adult mice. *A* is a wild type mouse. *B* is a SP-C (-/-) mouse[158].

Lamellar bodies maintain an internal acidic pH (around 6.0)[159] that is crucial for the processing of surfactant protein B and C[39] and for the correct lipids packaging prior to the release into the alveolar space[40]. A proton pump called Vacuolar ATPase or V-ATPase maintains the pH inside the lamellar bodies (Figure 2). V-ATPase is a multi-subunits enzyme that acidifies intracellular organelles (endosomes, lysosomes, secretory granules and synaptic vesicles) and is also present in the plasma membrane of macrophages, neutrophils, osteoclast and kidney intercalated cells (IC cells). Immune system cells use the V-ATPase

to maintain the cytosolic homeostasis when they reach acidic portions of the body like the inflammation sites. Osteoclasts acidify the extracellular matrix to dissolve the bone structure and to increase the activity of hydrolases, secreted by osteoclasts as well. IC cells in the kidney maintain the whole body acid/base balance through urine acidification.

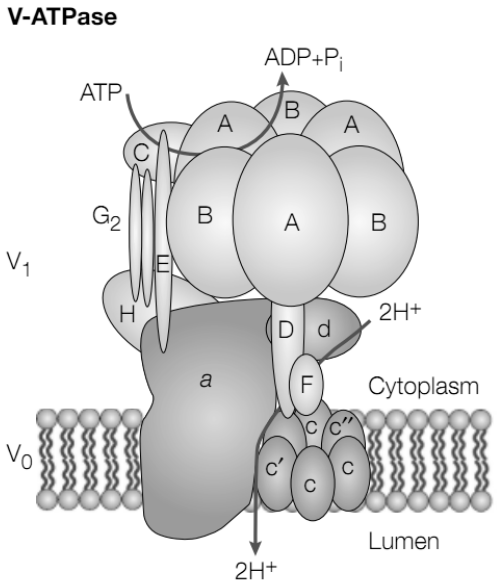

Figure 2. *Schematic representation of the V-ATPase. V0* is the intra-membrane part is, *V1* is the cytoplasmatic domain (adapted from Nishi et al. [160]).

The V-ATPase assembly of subunits allows the enzyme to act and localize differently. Some subunits are under or over expressed in particular tissue and this different distribution of subunits affects also the behavior of the enzyme[160]. For example a B1 knock out mouse maintains its phenotype in physiological condition but it is unable to completely recover from an acid load [161].

In this study we investigate the function of the B1 subunit of the V-ATPase focusing on IC cells as a model using a mouse model of B1-EGFP expressing mice. We compared wild type B1-EGFP and B1 knock out (but still expressing the EGFP on cells that could potentially express B1) mice to assess which structural variations affect the V-ATPase when the B1 subunit is silenced.

METHODS

Generation of the B1-EGFP mouse[162]

The EGFP coding region from the pEGFP-1 vector (Clontech, La Jolla, CA) was ligated into the vector containing 6.5 bp of the 5 -flanking region of the ATP6V1B1 gene. A polyadenylation signal from the SV40 virus early region with an added *Cla*I site was ligated into a site downstream from the EGFP coding region. This product was designated as pB1EGFPpA. Each plasmid intermediate and the final plasmid product were analyzed by performing PCR and restriction mapping to confirm the proposed structure. All ligation junctions were sequenced to confirm that the construct had the desired structure. The key elements are the 6.5-kb B1 promoter, 0.7-kb EGFP coding region, and 0.3-kb SV40 early region polyadenylation signal with unique *Cla*I sites upstream from the promoter and downstream from the polyadenylation sequence (Figure 3).

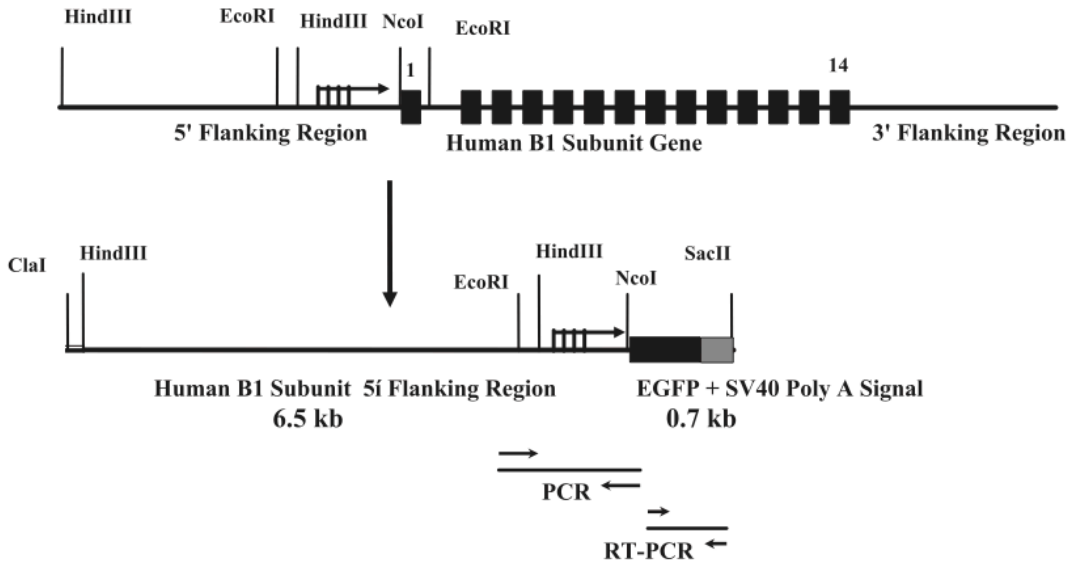

Figure 3. *The B1-EGFP transgene.* Human B1 V-ATPase gene is shown at top, hB1-EGFP transgene is shown at bottom. See text for details.

The B1-EGFP transgene was separated from the vector by agarose gel purification after digestion of pB1EGFPpA with *Cla*I. The DNA was isolated by electroelution, concentrated using an Elutip-D column (Schleicher & Schuell, Keene, NH), and resuspended in injection buffer consisting of 10 mM Tris, pH 7.4, and 0.1 mM EDTA. Transgenic mice were created by the University of Utah

transgenic mouse core facility using standard procedures as follows. The pronucleus of single-cell C57BL6 x CBA F1 embryos was microinjected with the purified transgene, and the resulting embryos were implanted into pseudopregnant females. The resulting pups were genotyped by performing PCR of tail DNA. The transgenic founders were each bred with C57BL/6 x CBA F1 mice. The resulting F1 and F2 animals were analyzed for expression of the transgene[163]. End-point PCR and Real Time PCR were used for genotyping and for analysis of transgene expression under standard conditions[162]. Primers and conditions are shown in Table 1.

Product	PCR Genotyping	Quantitative RT-PCR		Forward Primer
B1-EGFP	Yes		B1EGFPF	CCCTCTTCCCTTCTCCCTCCA
GAPDH		Yes	GAPDHF	CCTTCATTGACCTCAACTACATGG
B1		Yes	LCMB1F	ATCAATGTGCTCCCATCCCTCT
EGFP		Yes	LCEGFP	GCAGAAGAACGGCATCAAGG

Product	Temperature °C	Product Size bp		Reverse primer
B1-EGFP	63	366	BIEGFPR	CGCTGAACTTGTGGCCGTTT
GAPDH	57	442	GAPDHR	GCAGTGATGGCATGGACTGTGGT
B1	62	291	LCMB1R	AATGCGCTTCAGCATCTCTTTC
EGFP	62	333	LCEGFPR	GGGGAGGTGTGGGAGGTTTT

Table 1. *Primers and conditions for PCR and RT-PCR.*

Generation of the B1 (-/-) mouse[161]

Segments of the 129 SvJ murine *Atp6v1b1* genomic locus[164] were subcloned into Scrambler NTKV-1907 (Stratagene), replacing exons 7–11 with the Neo cassette. The 5 arm and 3 arms contained 8.3 and 1.7 kb of homology to the genomic locus, respectively. Linearized targeting vector was introduced into CJ7 mouse ES cells by electroporation. Genomic DNA from clones surviving double selection with G418 and ganciclovir was screened for a 2.1-kb PCR amplification product specific for the targeted *Atp6v1b1* locus; the forward primer was specific for the *Neo* cassette, and the reverse primer was specific for an *Atp6v1b1* 3' flanking sequence not included within the targeting vector. Homologous recombination was confirmed by Southern blotting of HindIII- and EcoRI-digested ES cell DNA with *Atp6v1b1* intron 1 and 3 flanking region probes, respectively.

Karyotypically normal targeted clones were injected into blastocysts to obtain chimeric mice, which were crossed with C57B/6 females to achieve germ-line transmission of the targeted allele in heterozygous, and ultimately homozygous, animals. Mice were genotyped by PCR using primer pairs specific for the wild type (intron/exon 9) and deleted alleles (*Neo* cassette) and genomic DNA as template. *Atp6v1b1* -/- mice derived from two independent targeted ES cell clones were phenotypically indistinguishable.

FACS isolation of B1-expressing cells from the kidney[165]

Mice were anesthetized using isoflurane. Kidneys were dissected and minced immediately with scissors in pre-warmed RPMI 1640 medium (Gibco Invitrogen, Carlsbad, CA) containing 1.0 mg/ml collagenase type I (Gibco Invitrogen), 1.0 mg/ml collagenase type II and 1.0 mg/ml hyaluronidase (Sigma Aldrich, St. Louis, MO). Tissue dissociation was performed for 45 min in a shaker (1400 rpm for 10 seconds every minute) 37°C. Cell preparations were then passed through a cell strainer with 40-µm nylon mesh to remove undigested material, and cells were washed once with RPMI 1640 medium and once with calcium-free phosphate-buffered saline (DPBS). Populations of EGFP-positive (EGFP+) cells from kidney preparation were isolated immediately by Fluorescence-Activated Cell Sorting (FACS) based on their green fluorescence intensity. Sorting was performed using a modified FACSVantage cell sorter (BD Biosciences, San Jose, CA) with DIVA option. EGFP+ and EGFP-negative (EGFP–) cell samples were collected in PBS or culture medium, and used without delay for protein isolation, RNA isolation, imaging or culture. Cells with intermediate to low fluorescence intensity were discarded to avoid potential contamination of cells that were negative for EGFP, but had a high autofluorescence, in the EGFP+ cell preparation. A fraction of each cell sample was reanalyzed by flow cytometry to estimate the purity (>95%). For RNA isolation, cell pellets were resuspended in RNA extraction buffer (RNeasy micro kit, Qiagen, Valencia, CA) and immediately processed.

Western Blot

For mice characterization, whole mouse kidneys were homogenized in RIPA buffer added with proteases inhibitor (Complete Mini, F. Hoffmann - La Roche Ltd, Basel, Switzerland) and centrifuged for 15 minutes at 13,000 x g at 4°C. For

positive cells analysis, 500,000 positive cells were obtained from the FACS from each mouse. Cells were then lysed in RIPA buffer added with proteases inhibitor (Complete Mini) as suggested by the manufacturer. Protein content was assessed by BCA assay (Thermo Fisher Scientific Inc., Rockford, IL, USA). Ten ug of proteins were loaded in well of a 4-20% PAGE gel (10 wells, 50 ul each, Biorad, Hercules, CA, USA) with Laemmli buffer (Biorad, reducing condition) as suggested by manufacturer.

Immunoblotting was carried out using a rabbit V-ATPase A, E and B1-subunits polyclonal antibodies (1:1,000), and horseradish peroxidase-conjugated donkey anti-rabbit IgG (1:5,000, Jackson ImmunoResearch, West Grove, PA, USA). Chicken V-ATPase B2-subunit polyclonal antibody (1:1,000), and horseradish peroxidase-conjugated donkey anti-chicken IgY (1:5,000, Jackson ImmunoResearch). Run and transfer were performed as suggested in a Biorad apparatus (Mini Protean) [161]. Monoclonal anti-mouse Actin (1:20,000, Sigma-Aldrich, St. Louis, MO, USA), and donkey anti-mouse IgG (1:5,000, Jackson ImmunoResearch).

Data Analysis

Images were processed and quantified with ImageJ software.

RESULTS

Generation of the B1-EGFP mouse

The V-ATPase B1-subunit gene (6.5 kb, ATP6V1B1 gene; Gen- Bank accession no. NM_039350) 5' -flanking region was used to drive expression of an EGFP expression cassette (Clontech). The transgene includes the 5' -flanking region of the ATP6V1B1 gene extending to but excluding the endogenous translational start codon. The EGFP cassette includes the EGFP coding region, with its own translational start site, and an SV40 polyadenylation signal. Oligonucleotide primers were designed to anneal to the promoter and EGFP coding region to perform PCR genotyping. Primers were also designed to anneal within the EGFP coding region to perform RT-PCR analysis. The transgene minus the vector backbone is referred to as B1- EGFP. The B1-EGFP transgene was used to create transgenic mice. Pro-nuclear microinjections and embryo implantation

was per- formed by the University of Utah Transgenic Mouse Core Facility using standard methods. Approximately 50 live pups were analyzed for the presence of the B1-EGFP transgene by performing PCR analysis of tail DNA. Oligonucleotide primers and conditions of PCR are shown in Table 1. The integrity of tail DNA was verified using PCR with primers specific for the endogenous mouse aquaporin type 2 (AQP2) gene (GenBank accession no. NT_039621). Six founders containing the B1-EGFP transgene were identified (Figure 4). Trans- gene levels in the founders were estimated by comparing the intensity of PCR products to that observed for nontransgenic mouse DNA spiked with 0, 1, 10, and 100 copies per cell equivalent of the transgene. Founders F1, F3, F16, and F43 appear to have at least 100 copies per cell equivalent of the transgene, while founders F39 and F40 have 10 copies. All founders were crossed with wild-type C57BL/6 X CBA F1 mice and hemizygous offspring analyzed for expression of the transgene. Offspring derived from the F1 and F16 founders are referred to as lines 1 and 3, respectively. They demonstrated kidney, epididymis, and lung expression of the B1-EGFP transgene and continued to do so in the F1, F2, and F3 generations. One additional line exhibited expression of the B1-EGFP transgene in a pattern that was consistent with collecting duct expression, but the expression was incomplete and therefore was not fully characterized.

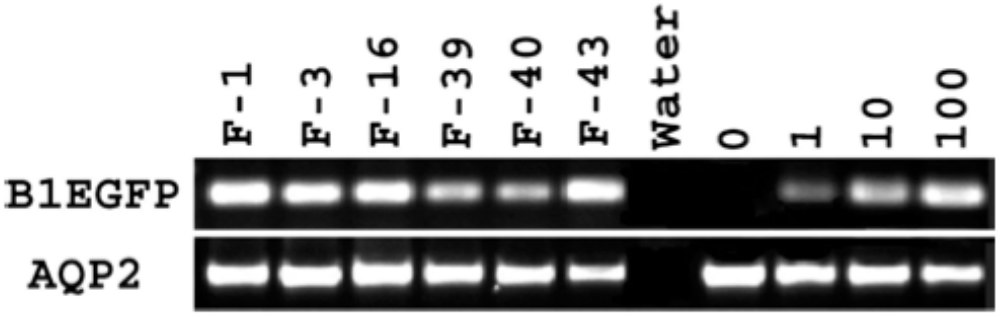

Figure 2. *PCR genotyping of mouse tail DNA*. hB1-EGFP transgene was present in six founder mice. Transgenic tail DNA (left) and normal mouse DNA spiked with 0, 1, 10, and 100 copies per cell equivalent of the purified transgene DNA (right) were amplified by PCR using primers specific for the hB1-EGFP transgene (top) and the endogenous murine aquaporin type 2 gene (AQP2; bottom).

Generation of the B1 (-/-) mouse

The murine *Atp6v1b1* genomic locus in CJ7 ES cells was disrupted by replacing exons 7–11 with a neomycin resistance cassette via homologous recombination (Figure 5a). Because missense mutations in these exons are sufficient to eliminate normal gene product function, their deletion is anticipated to do the same. Screening of ES cell DNA of 211 clones surviving selection with G418 and ganciclovir identified two clones that yielded a PCR amplification product specific for the targeted *Atp6v1b1* genomic locus (data not shown; see Methods). Homologous recombination of both arms of the targeting vector was confirmed in these clones by Southern blotting (Figure 5 b and c).

Targeted clones were injected into blastocysts to generate *Atp6v1b1* +/- chimeric mice; chimeric males were, in turn, bred with C57B 6 females. Tail DNAs of the resulting agouti off- spring were screened by PCR to identify germline transmission of the mutant allele, and lines established from both ES clones transmitted the disrupted allele. Intercrossing of *Atp6v1b1+/-* mice yielded offspring of all three genotypes (Figure 5d) in expected Mendelian ratios; there was no evidence for decreased fetal or neonatal viability of *Atp6v1b1* -/- mice. *Atp6v1b1* -/- mice raised on a standard diet were fully fertile and showed normal growth and behavior when followed up to 1 year of age.

Western blotting showed that B1-subunit expression was absent in whole kidney homogenates of *Atp6v1b1* -/- mice (Figure 5e)[161].

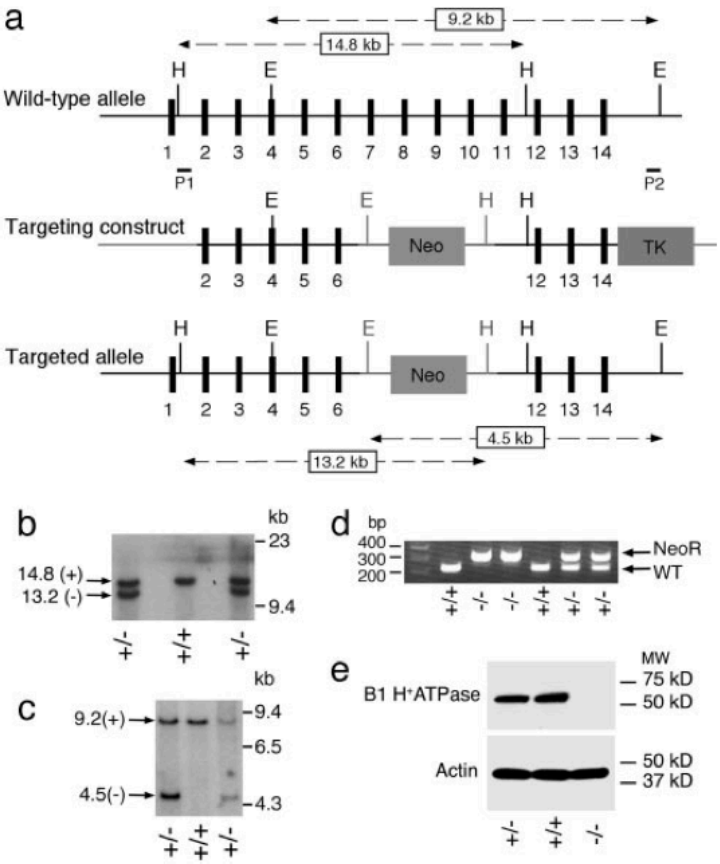

Figure 5. *Generation of H ATPase B1-subunit deficient mice.* (a) Structure of the endogenous locus, targeting construct and targeted allele are shown. The segments not endogenous to the WT allele are shown in gray. Numbered boxes represent exons of *Atp6v1b1*. The sizes of restriction fragments resulting from HindIII (H) and EcoRI (E) digestion of the WT and targeted alleles, and the locations of probes (P1, P2) used for Southern blotting are shown. "Neo" denotes neomycin resistance gene; "TK" denotes thymidine kinase gene. (b and c) Confirmation of *Atp6v1b1* gene targeting. Genomic DNA of WT (+/+) or heterozygous (+/-) targeted deletion ES cell lines were digested with indicated enzymes, fractionated on 0.8% agarose gels, and subjected to Southern blotting. (b) Hybridization of probe P1 to HindIII-digested DNA is shown. (c) Hybridization of probe P2 to EcoRI-digested DNA is shown. Fragments corresponding to the targeted (-) alleles are seen only in targeted clones. (d) Genotyping of Atp6v1b1 in +/+, +/-, and -/- mice. PCR of genomic DNA was performed by using primer pairs specific for the WT (intronexon 9) and deleted alleles (Neo cassette) and genomic DNA as template (see Methods). Products were resolved on a 2% agarose gel. The inferred genotypes are indicated. (e) Immunoblotting of total kidney homogenates with antibodies to the B1-subunit was performed (see Methods). Expression is seen in *Atp6v1b1+/+* and *Atp6v1b1 +/-* mice, but is absent in *Atp6v1b1 -/-* mice.

FACS isolation of B1-expressing cells from the kidney

The average percentage of positive isolated cells was 2-5%. Cells population was confirmed to consist of pure and viable Intercalated Cells (IC) as described by previous experiments [162,165] with immunohistochemistry and electron microscope.

Western Blotting of FACS-isolated IC Cells

As purity of the cell populations was mandatory for the biological significance, the presence of AQP2 was assessed in all the samples used for western blotting. AQP2 is a specific marker of kidney principal cells (the most abundant type of kidney cells). Samples resulted all AQP2-free (Figure 6). B1 knock out cells resulted also free of B1 staining (Figure 7).

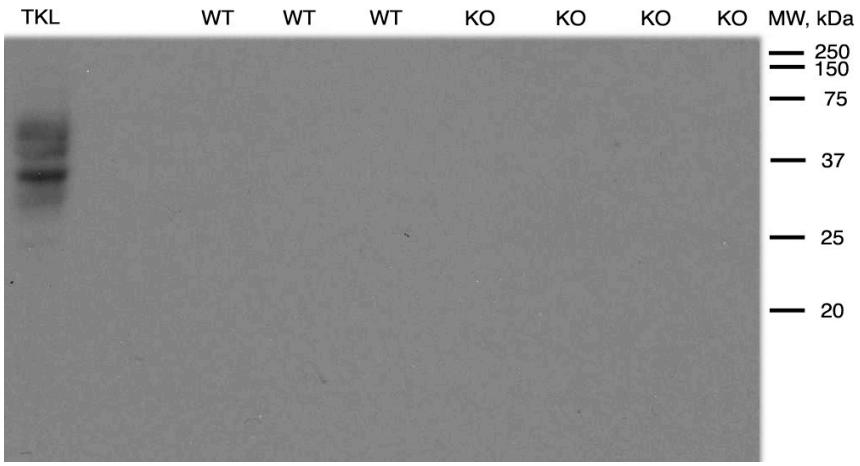

Figure 6. *AQP2 staining of EGFP+ IC cells*. WT are wild type B1-EGFP cells. KO are knock out B1-EGFP cells. TLK is mouse total kidney lysate from a pure wild type (no B1-EGFP). Actin staining is shown below.

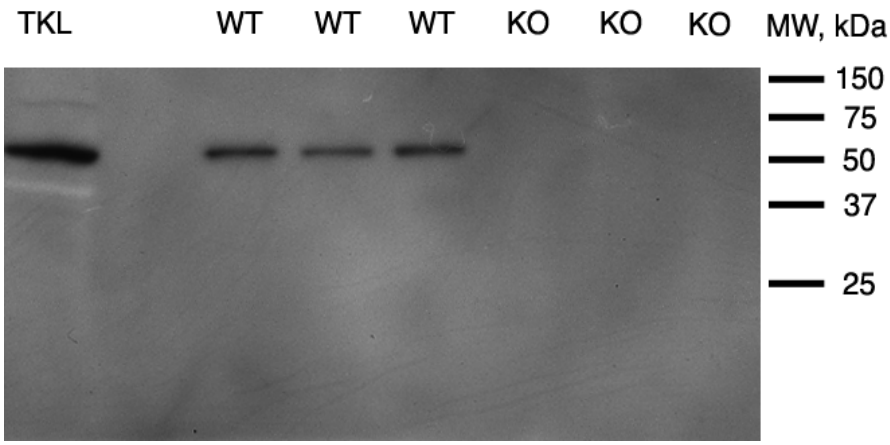

Figure 7. *B1 subunit staining of EGFP+ IC cells.* WT are wild type B1-EGFP cells. KO are knock out B1-EGFP cells. TLK is mouse total kidney lysate from a pure wild type (no B1-EGFP).

After assessing the purity we tested the modification of A, B2 and E subunits of the V-ATPase. Subunits' A and E content decrease in KO mice, while B2 increases (Figures 8 to 12).

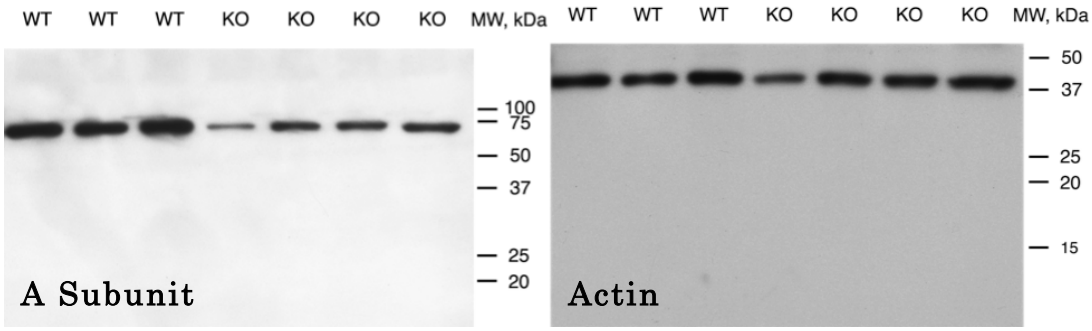

Figure 8. *A subunit staining of EGFP+ IC cells.* WT are wild type B1-EGFP cells. KO are knock out B1-EGFP cells. TLK is mouse total kidney lysate from a pure wild type (no B1-EGFP).

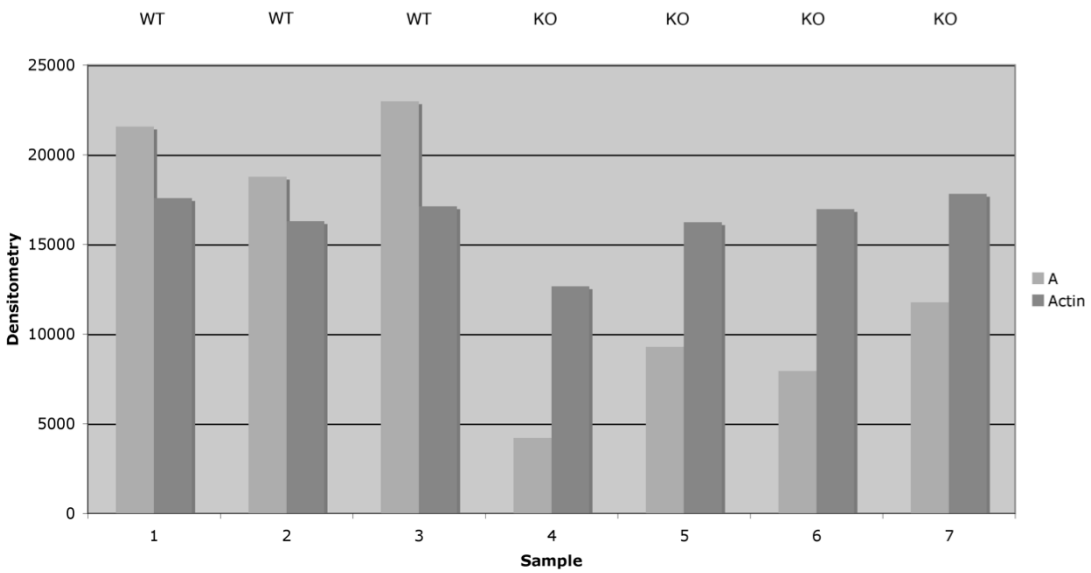

Figure 9. *A subunit densitometry*. Subunit A bars are normalized to actin.

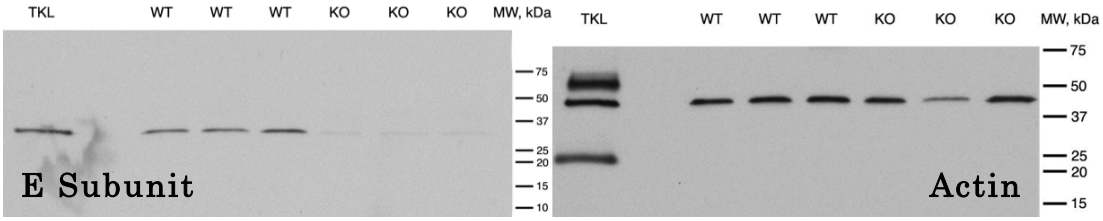

Figure 10. *E subunit staining of EGFP+ IC cells*. WT are wild type B1-EGFP cells. KO are knock out B1-EGFP cells. TLK is mouse total kidney lysate from a pure wild type (no B1-EGFP).

Densitometry of A, E and B2 were calculated with the function "Gel" of ImageJ software.

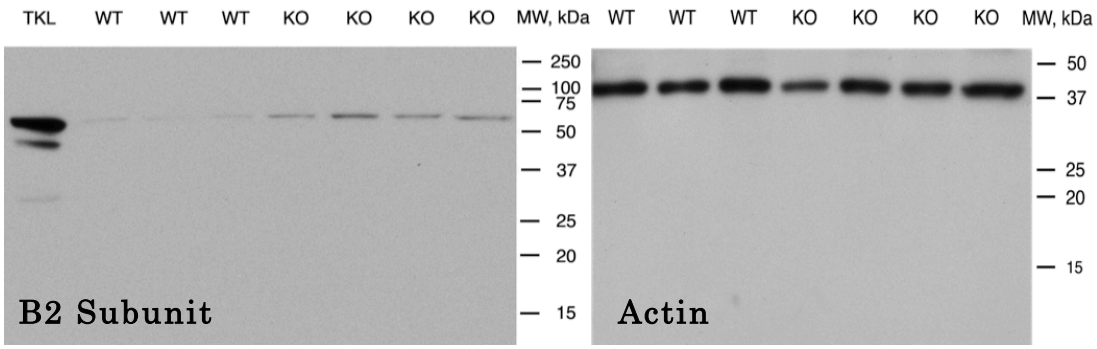

Figure 11. *B2 subunit staining of EGFP+ IC cells.* WT are wild type B1-EGFP cells. KO are knock out B1-EGFP cells. TLK is mouse total kidney lysate from a pure wild type (no B1-EGFP). B2 subunit is upregulated in B1 deficient mice.

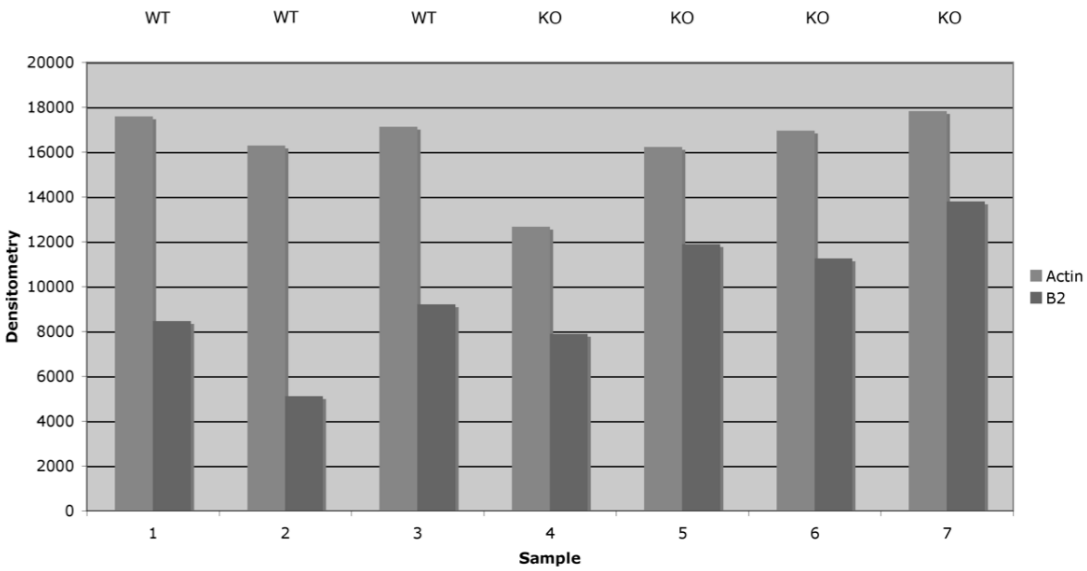

Figure 12. *B2 subunit densitometry.* Subunit B2 bars are normalized to actin.

DISCUSSION

The V-ATPase is the main mediator of renal H^+ secretion and it is crucial for the regulation of body acid-base balance. Even in the lungs V-ATPase role is now being thought as fundamental for surfactant secretion[41]. We generated a mouse breed that express EGFP in the cells that also express the B1 subunit of the V-ATPase. Such cells are located in the kidney (intercalated cells), in the olfactory system, in the male reproductive tract and in the lungs (not fully characterized epithelial cells). Because of the experience of the Brown laboratory on kidney cells, we focused on intercalated cells to understand the mechanism of action and regulation of V-ATPase in intercalated cells to create the basis for further studies on the V-ATPase in the other tissues like the lungs. We cross B1-EGFP expressing mice with B1 knock out (-/-) to generate a B1 (-/-) EGFP breed that express EGFP in cells where B1 should have been, but not expressed (Figure 13).

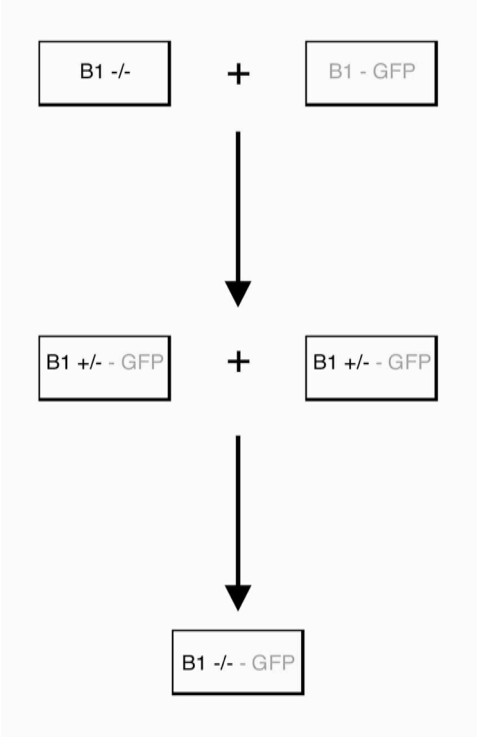

Figure 13. *Generation of the B1 (-/-) EGFP mice breed.* B1-EGFP mice where crossed with B1 (-/-) mice to generate a hybrid population.

Deficiencies in V-ATPase activity underlie a number of diseases (such as distal Renal Tubular Acidosis, Fanconi syndrome, nephrolithiasis) RTAs can have

genetic or acquired causes; mutations in the B1 and a4 subunits of the V-ATPase are a main cause of dRTA and, in certain cases, hearing loss.

In this study we isolated by flow cytometry (FACS) a pure population of IC cells from wild type mice and from B1 knock out mice, and we investigate why B1 deficient mice have a normal phenotype under normal condition but they can not successfully handle an acid load[161]. We found that unlike previously reported[166], that the increased compensatory apical B2 expression is not only due to redistribution, but there is an actual upregulation of B2 at the protein level. There is also an overall downregulation of V-ATPase expression (downregulation of A and E subunits), which matches very well the previously reported decrease in V-ATPase activity (Table 2).

V-ATPase subunit	**Wild type** mice Mean ± SE (n=3)	**B1-deficient** mice Mean ± SE (n=4)
B2	1.000 ± 0.151	1.572 ± 0.076
A	1.000 ± 0.044	0.409 ± 0.057
E	1.000 ± 0.034	0.408 ± 0.113

WT: Vtot = VB1 + VB2
KO: Vtot * 0.4 = VB2 * 1.6

=> VB1 = Vtot * 0.75
VB2 = Vtot * 0.25
VB1 / VB2 = 3

Table 2. *Mathematical model of V-ATPase subunit up/down-regulation in B1-deficient mice*. In the B1 deficient mouse, V-ATPase machinery is maintained by a 3 times increase of the B2 subunit, while all the other subunits decreases each of the same amount.

The upregulation of B2 compensates for the lack of B1, and is sufficient to maintain acid-base homeostasis under baseline conditions, even when other V-ATPase subunits are downregulated. As reported before, we did not find any variation (measure with RT-PCR) in the mRNA amount encoding for each subunit[166]. As having no change in mRNA levels does not preclude a change at the protein level, we speculate that the gene translation can be regulated differently, or the subunits degradation rate might be different in the knock out mice (or both).

Is not known if mutations in the V-ATPase subunits can give rise to lung diseases. C2-a subunit is specifically expressed in the lamellar bodies of the lungs[167] but its function (together with its kidney specific splice variant C2-b) is unknown. Further studies are needed to unveil the biological significance of these findings, in particular in the lungs where almost nothing is known on the V-ATPase role in surfactant homeostasis.

This study was submitted for publication.

Acknowledgements

LV would like to thank Manuela Simonato, Maddalena Facco, Ilena Isak, Giulia Lamonica, Paola E. Cogo and Virgilio P. Carnielli from the Padua Critical Care Lab for their fundamental help doing this thesis.

Teodor Paunescu, Dennis Brown, Sylvie Breton, John Rothermel, Valentina Vaja, Nicolas Da Silva, Richard Bouley, William Rice, Jeremy Roy, Shan Zhuo Chan, Eric Hill, Margaret McLaughlin, Delphine Maynard-Sautet, Chia Chi Sun, Sandra Chen, Matthew Weber, Dennis Ausiello, Ying Chen, Maria Merkulova, Quifang Wu, Robert Tyszkowski, Jianxin Zhu, Herbert Lin, Jenny Lu and all the Boston PMB Lab for the fantastic work that we carried out together.

References

1. Notter RH. Introduction to surface tension and Surfactants. In: Lenfant C, ed. *Lung Surfactants: Basic Science and Clinical Applications.* Vol 149. New York: Marcel Dekker Inc.; 2000.
2. Hawgood S, Clements JA. Pulmonary surfactant and its apoproteins. *J Clin Invest.* Jul 1990;86(1):1-6.
3. Notter RH, Finkelstein JN. Pulmonary surfactant: an interdisciplinary approach. *J Appl Physiol.* Dec 1984;57(6):1613-1624.
4. Froh D, Ballard PL, Williams MC, et al. Lamellar bodies of cultured human fetal lung: content of surfactant protein A (SP-A), surface film formation and structural transformation in vitro. *Biochim Biophys Acta.* Apr 9 1990;1052(1):78-89.
5. Haagsman HP, Sargeant T, Hauschka PV, Benson BJ, Hawgood S. Binding of calcium to SP-A, a surfactant-associated protein. *Biochemistry.* Sep 25 1990;29(38):8894-8900.
6. Williams MC. Conversion of lamellar body membranes into tubular myelin in alveoli of fetal rat lungs. *J Cell Biol.* Feb 1977;72(2):260-277.
7. Williams MC. Ultrastructure of tubular myelin and lamellar bodies in fast-frozen adult rat lung. *Exp Lung Res.* Dec 1982;4(1):37-46.
8. Ikegami M, Korfhagen TR, Whitsett JA, et al. Characteristics of surfactant from SP-A-deficient mice. *Am J Physiol.* Aug 1998;275(2 Pt 1):L247-254.
9. Cockshutt AM, Weitz J, Possmayer F. Pulmonary surfactant-associated protein A enhances the surface activity of lipid extract surfactant and reverses inhibition by blood proteins in vitro. *Biochemistry.* Sep 11 1990;29(36):8424-8429.
10. Wang Z, Hall SB, Notter RH. Roles of different hydrophobic constituents in the adsorption of pulmonary surfactant. *J Lipid Res.* Apr 1996;37(4):790-798.
11. Notter RH. Functional Composition and Component Biophysics. In: Lenfant C, ed. *Lung Surfactants: Basic Science and Clinical Applications.* Vol 149. New York: Marcel Dekker Inc.; 2000:199-201.

12. Crouch EC. Collectins and pulmonary host defense. *Am J Respir Cell Mol Biol.* Aug 1998;19(2):177-201.
13. Haagsman HP. Surfactant proteins A and D. *Biochem Soc Trans.* Feb 1994;22(1):100-106.
14. Mason RJ, Greene K, Voelker DR. Surfactant protein A and surfactant protein D in health and disease. *Am J Physiol.* Jul 1998;275(1 Pt 1):L1-13.
15. Chinoy MR. Embryology of the Lungs. In: Shields TWLJR, C.E. Feins, R.H., ed. *General Thoracic Surgery, 7th Edition.* Vol 1: Lippincott Williams & Wilkins; 2009.
16. Ikegami M. Surfactant catabolism. *Respirology.* Jan 2006;11 Suppl:S24-27.
17. Batenburg JJ. Surfactant phospholipids: synthesis and storage. *Am J Physiol.* Apr 1992;262(4 Pt 1):L367-385.
18. Haagsman HP, van Golde LM. Synthesis and assembly of lung surfactant. *Annu Rev Physiol.* 1991;53:441-464.
19. Rooney SA. The surfactant system and lung phospholipid biochemistry. *Am Rev Respir Dis.* Mar 1985;131(3):439-460.
20. van Golde LM, Casals CC. Metabolism of Lipids. In: Crystal RG, West JB, Weibel ER, Barnes PJ, eds. *The Lung: Scientific Foundations 2nd Edition*. Philadelphia: Lippincott-Raven; 1997:9-18.
21. Anceschi MM, Di Renzo GC, Venincasa MD, Bleasdale JE. The choline-depleted type II pneumonocyte. A model for investigating the synthesis of surfactant lipids. *Biochem J.* Nov 15 1984;224(1):253-262.
22. Bleasdale JE, Tyler NE, Snyder JM. Subcellular sites of synthesis of phosphatidylglycerol and phosphatidylinositol in type II pneumonocytes. *Lung.* 1985;163(6):345-359.
23. Quirk JG, Bleasdale JE, MacDonald PC, Johnston JM. A role for cytidine monophosphate in the regulation of the glycerophospholipid composition of surfactant in developing lung. *Biochem Biophys Res Commun.* Aug 14 1980;95(3):985-992.
24. Batenburg JJ, Haagsman HP. The lipids of pulmonary surfactant: dynamics and interactions with proteins. *Prog Lipid Res.* Sep 1998;37(4):235-276.

25. Wong CJ, Akiyama J, Allen L, Hawgood S. Localization and developmental expression of surfactant proteins D and A in the respiratory tract of the mouse. *Pediatr Res.* Jun 1996;39(6):930-937.
26. Walker SR, Williams MC, Benson B. Immunocytochemical localization of the major surfactant apoproteins in type II cells, Clara cells, and alveolar macrophages of rat lung. *J Histochem Cytochem.* Sep 1986;34(9):1137-1148.
27. Voorhout WF, Veenendaal T, Haagsman HP, et al. Intracellular processing of pulmonary surfactant protein B in an endosomal/lysosomal compartment. *Am J Physiol.* Oct 1992;263(4 Pt 1):L479-486.
28. Liggins GC, Howie RN. A controlled trial of antepartum glucocorticoid treatment for prevention of the respiratory distress syndrome in premature infants. *Pediatrics.* Oct 1972;50(4):515-525.
29. Mason RJ, Lewis MC, Edeen KE, McCormick-Shannon K, Nielsen LD, Shannon JM. Maintenance of surfactant protein A and D secretion by rat alveolar type II cells in vitro. *Am J Physiol Lung Cell Mol Physiol.* Feb 2002;282(2):L249-258.
30. Mason RJ, Voelker DR. Regulatory mechanisms of surfactant secretion. *Biochim Biophys Acta.* Nov 19 1998;1408(2-3):226-240.
31. Dietl P, Haller T, Mair N, Frick M. Mechanisms of surfactant exocytosis in alveolar type II cells in vitro and in vivo. *News Physiol Sci.* Oct 2001;16:239-243.
32. Jobe A. Metabolism of endogenous surfactant and exogenous surfactants for replacement therapy. *Semin Perinatol.* Jul 1988;12(3):231-244.
33. Jacobs H, Jobe A, Ikegami M, Jones S. Surfactant phosphatidylcholine source, fluxes, and turnover times in 3-day-old, 10-day-old, and adult rabbits. *J Biol Chem.* Feb 25 1982;257(4):1805-1810.
34. Nicholas TE, Power JH, Barr HA. Surfactant homeostasis in the rat lung during swimming exercise. *J Appl Physiol.* Dec 1982;53(6):1521-1528.
35. Nicholas TE, Power JH, Barr HA. The pulmonary consequences of a deep breath. *Respir Physiol.* Sep 1982;49(3):315-324.
36. Wright JR, Dobbs LG. Regulation of pulmonary surfactant secretion and clearance. *Annu Rev Physiol.* 1991;53:395-414.
37. Chander A. Regulation of lung surfactant secretion by intracellular pH. *Am J Physiol.* Dec 1989;257(6 Pt 1):L354-360.

38. Mason RJ, Cott GR, Robinson PC, Sugahara K, Leslie C, Dobbs LG. Pharmacology of alveolar type II cells. *Prog Respir Res.* 1984(18):279-287.
39. Beers MF. Inhibition of cellular processing of surfactant protein C by drugs affecting intracellular pH gradients. *J Biol Chem.* Jun 14 1996;271(24):14361-14370.
40. Chander A, Sen N, Wu AM, Higgins S, Wadsworth S, Spitzer AR. Methylamine decreases trafficking and packaging of newly synthesized phosphatidylcholine in lamellar bodies in alveolar type II cells. *Biochem J.* Aug 15 1996;318 (Pt 1):271-278.
41. Chintagari NR, Mishra A, Su L, et al. Vacuolar ATPase regulates surfactant secretion in rat alveolar type II cells by modulating lamellar body calcium. *PLoS One.* 2010;5(2):e9228.
42. Dobbs LG, Wright JR, Hawgood S, Gonzalez R, Venstrom K, Nellenbogen J. Pulmonary surfactant and its components inhibit secretion of phosphatidylcholine from cultured rat alveolar type II cells. *Proc Natl Acad Sci U S A.* Feb 1987;84(4):1010-1014.
43. Wright JR, Wager RE, Hawgood S, Dobbs L, Clements JA. Surfactant apoprotein Mr = 26,000-36,000 enhances uptake of liposomes by type II cells. *J Biol Chem.* Feb 25 1987;262(6):2888-2894.
44. Haagsman HP, Hawgood S, Sargeant T, et al. The major lung surfactant protein, SP 28-36, is a calcium-dependent, carbohydrate-binding protein. *J Biol Chem.* Oct 15 1987;262(29):13877-13880.
45. Kuroki Y, Shiratori M, Murata Y, Akino T. Surfactant protein D (SP-D) counteracts the inhibitory effect of surfactant protein A (SP-A) on phospholipid secretion by alveolar type II cells. Interaction of native SP-D with SP-A. *Biochem J.* Oct 1 1991;279 (Pt 1):115-119.
46. Fisher AB, Dodia C, Chander A. Secretagogues for lung surfactant increase lung uptake of alveolar phospholipids. *Am J Physiol.* Oct 1989;257(4 Pt 1):L248-252.
47. Brown LA, Pasquale SM, Longmore WJ. Role of microtubules in surfactant secretion. *J Appl Physiol.* Jun 1985;58(6):1866-1873.
48. Dobbs LG, Mason RJ. Stimulation of secretion of disaturated phosphatidylcholine from isolated alveolar type II cells by 12-O-

tetradecanoyl-13-phorbol acetate. *Am Rev Respir Dis.* Oct 1978;118(4):705-733.

49. Gurel O, Ikegami M, Chroneos ZC, Jobe AH. Macrophage and type II cell catabolism of SP-A and saturated phosphatidylcholine in mouse lungs. *Am J Physiol Lung Cell Mol Physiol.* Jun 2001;280(6):L1266-1272.
50. Rider ED, Ikegami M, Jobe AH. Intrapulmonary catabolism of surfactant-saturated phosphatidylcholine in rabbits. *J Appl Physiol.* Nov 1990;69(5):1856-1862.
51. Ikegami M, Ueda T, Hull W, et al. Surfactant metabolism in transgenic mice after granulocyte macrophage-colony stimulating factor ablation. *Am J Physiol.* Apr 1996;270(4 Pt 1):L650-658.
52. Reed JA, Ikegami M, Robb L, Begley CG, Ross G, Whitsett JA. Distinct changes in pulmonary surfactant homeostasis in common beta-chain- and GM-CSF-deficient mice. *Am J Physiol Lung Cell Mol Physiol.* Jun 2000;278(6):L1164-1171.
53. Ikegami M, Dhami R, Schuchman EH. Alveolar lipoproteinosis in an acid sphingomyelinase-deficient mouse model of Niemann-Pick disease. *Am J Physiol Lung Cell Mol Physiol.* Mar 2003;284(3):L518-525.
54. Williams MC. Endocytosis in alveolar type II cells: effect of charge and size of tracers. *Proc Natl Acad Sci U S A.* Oct 1984;81(19):6054-6058.
55. Jacobs HC, Ikegami M, Jobe AH, Berry DD, Jones S. Reutilization of surfactant phosphatidylcholine in adult rabbits. *Biochim Biophys Acta.* Oct 23 1985;837(1):77-84.
56. Jacobs HC, Jobe AH, Ikegami M, Jones S. Reutilization of phosphatidylglycerol and phosphatidylethanolamine by the pulmonary surfactant system in 3-day-old rabbits. *Biochim Biophys Acta.* Apr 25 1985;834(2):172-179.
57. Chander A, Claypool WD, Jr., Strauss JF, 3rd, Fisher AB. Uptake of liposomal phosphatidylcholine by granular pneumocytes in primary culture. *Am J Physiol.* Nov 1983;245(5 Pt 1):C397-404.
58. Kishore U, Greenhough TJ, Waters P, et al. Surfactant proteins SP-A and SP-D: structure, function and receptors. *Mol Immunol.* Mar 2006;43(9):1293-1315.

59. Rice WR, Sarin VK, Fox JL, Baatz J, Wert S, Whitsett JA. Surfactant peptides stimulate uptake of phosphatidylcholine by isolated cells. *Biochim Biophys Acta.* Nov 28 1989;1006(2):237-245.

60. Korfhagen TR, Sheftelyevich V, Burhans MS, et al. Surfactant protein-D regulates surfactant phospholipid homeostasis in vivo. *J Biol Chem.* Oct 23 1998;273(43):28438-28443.

61. Ikegami M, Whitsett JA, Jobe A, Ross G, Fisher J, Korfhagen T. Surfactant metabolism in SP-D gene-targeted mice. *Am J Physiol Lung Cell Mol Physiol.* Sep 2000;279(3):L468-476.

62. Ikegami M, Hull WM, Yoshida M, Wert SE, Whitsett JA. SP-D and GM-CSF regulate surfactant homeostasis via distinct mechanisms. *Am J Physiol Lung Cell Mol Physiol.* Sep 2001;281(3):L697-703.

63. Ogasawara Y, Kuroki Y, Akino T. Pulmonary surfactant protein D specifically binds to phosphatidylinositol. *J Biol Chem.* Oct 15 1992;267(29):21244-21249.

64. Persson AV, Gibbons BJ, Shoemaker JD, Moxley MA, Longmore WJ. The major glycolipid recognized by SP-D in surfactant is phosphatidylinositol. *Biochemistry.* Dec 8 1992;31(48):12183-12189.

65. Poulain FR, Akiyama J, Allen L, et al. Ultrastructure of phospholipid mixtures reconstituted with surfactant proteins B and D. *Am J Respir Cell Mol Biol.* May 1999;20(5):1049-1058.

66. Jobe AH, Ikegami M. Surfactant metabolism. *Clin Perinatol.* Dec 1993;20(4):683-696.

67. Ikegami M, Jobe AH. Surfactant metabolism. *Semin Perinatol.* Aug 1993;17(4):233-240.

68. Holm BA, Enhorning G, Notter RH. A biophysical mechanism by which plasma proteins inhibit lung surfactant activity. *Chem Phys Lipids.* Nov 1988;49(1-2):49-55.

69. Holm BA, Wang Z, Notter RH. Multiple mechanisms of lung surfactant inhibition. *Pediatr Res.* Jul 1999;46(1):85-93.

70. Pison U, Tam EK, Caughey GH, Hawgood S. Proteolytic inactivation of dog lung surfactant-associated proteins by neutrophil elastase. *Biochim Biophys Acta.* Sep 15 1989;992(3):251-257.

71. Hack M, Horbar JD, Malloy MH, Tyson JE, Wright E, Wright L. Very low birth weight outcomes of the National Institute of Child Health and

Human Development Neonatal Network. *Pediatrics.* May 1991;87(5):587-597.

72. Hulsey TC, Alexander GR, Robillard PY, Annibale DJ, Keenan A. Hyaline membrane disease: the role of ethnicity and maternal risk characteristics. *Am J Obstet Gynecol.* Feb 1993;168(2):572-576.

73. Avery ME, Mead J. Surface properties in relation to atelectasis and hyaline membrane disease. *AMA J Dis Child.* May 1959;97(5, Part 1):517-523.

74. Crystal RG, West JB, Weibel ER, Barnes PJ. *The Lung: Scientific Foundations*. Vol 1, 2. Philadelphia: Lippincott-Raven; 1997.

75. Kumar V, Cotran RS, Robbins SL. *Basic Pathology*. 6th ed. Philadelphia: WB Saunders; 1997.

76. Bernard GR, Artigas A, Brigham KL, et al. The American-European Consensus Conference on ARDS. Definitions, mechanisms, relevant outcomes, and clinical trial coordination. *Am J Respir Crit Care Med.* Mar 1994;149(3 Pt 1):818-824.

77. Hall JB, Schmidt GA, Wood LDH. *Principles of critical care*. 3rd ed. New York: McGraw-Hill, Medical Pub. Division; 2005.

78. Davis SL, Furman DP, Costarino AT, Jr. Adult respiratory distress syndrome in children: associated disease, clinical course, and predictors of death. *J Pediatr.* Jul 1993;123(1):35-45.

79. Taussig LM, Landau LI, P.N. LS, W.J. M, Martinez FD, Sly PD. *Pediatric Respiratory Medicine*. St. Louis: Mosby; 1999.

80. Gregory TJ, Longmore WJ, Moxley MA, et al. Surfactant chemical composition and biophysical activity in acute respiratory distress syndrome. *J Clin Invest.* Dec 1991;88(6):1976-1981.

81. Koletzko S, Haisch M, Seeboth I, et al. Isotope-selective non-dispersive infrared spectrometry for detection of Helicobacter pylori infection with 13C-urea breath test. *Lancet.* Apr 15 1995;345(8955):961-962.

82. Wolfe RR, Chinkes DL. *Isotope tracers in metabolic research : principles and practice of kinetic analysis*. 2nd ed. Hoboken, N.J.: Wiley-Liss; 2005.

83. Koletzko B, Demmelmair H, Hartl W, et al. The use of stable isotope techniques for nutritional and metabolic research in paediatrics. *Early Hum Dev.* Dec 1998;53 Suppl:S77-97.

84. Jones PJ, Leatherdale ST. Stable isotopes in clinical research: safety reaffirmed. *Clin Sci (Lond).* Apr 1991;80(4):277-280.

85. Cogo PE, Carnielli VP, Bunt JE, et al. Endogenous surfactant metabolism in critically ill infants measured with stable isotope labeled fatty acids. *Pediatr Res.* Feb 1999;45(2):242-246.

86. Cogo PE, Simonato M, Mariatoffolo G, et al. Dexamethasone therapy in preterm infants developing bronchopulmonary dysplasia: effect on pulmonary surfactant disaturated-phosphatidylcholine kinetics. *Pediatr Res.* Apr 2008;63(4):433-437.

87. Cogo PE, Toffolo GM, Ori C, et al. Surfactant disaturated-phosphatidylcholine kinetics in acute respiratory distress syndrome by stable isotopes and a two compartment model. *Respir Res.* 2007;8:13.

88. Cogo PE, Zimmermann LJ, Meneghini L, et al. Pulmonary surfactant disaturated-phosphatidylcholine (DSPC) turnover and pool size in newborn infants with congenital diaphragmatic hernia (CDH). *Pediatr Res.* Nov 2003;54(5):653-658.

89. Cogo PE, Zimmermann LJ, Pesavento R, et al. Surfactant kinetics in preterm infants on mechanical ventilation who did and did not develop bronchopulmonary dysplasia. *Crit Care Med.* May 2003;31(5):1532-1538.

90. Cogo PE, Zimmermann LJ, Rosso F, et al. Surfactant synthesis and kinetics in infants with congenital diaphragmatic hernia. *Am J Respir Crit Care Med.* Jul 15 2002;166(2):154-158.

91. Cogo PE, Zimmermann LJ, Verlato G, et al. A dual stable isotope tracer method for the measurement of surfactant disaturated-phosphatidylcholine net synthesis in infants with congenital diaphragmatic hernia. *Pediatr Res.* Aug 2004;56(2):184-190.

92. Janssen DJ, Carnielli VP, Cogo PE, et al. Surfactant phosphatidylcholine half-life and pool size measurements in premature baboons developing bronchopulmonary dysplasia. *Pediatr Res.* Nov 2002;52(5):724-729.

93. Verlato G, Cogo PE, Balzani M, et al. Surfactant status in preterm neonates recovering from respiratory distress syndrome. *Pediatrics.* Jul 2008;122(1):102-108.

94. Verlato G, Cogo PE, Benetti E, Gomirato S, Gucciardi A, Carnielli VP. Kinetics of surfactant in respiratory diseases of the newborn infant. *J Matern Fetal Neonatal Med.* Nov 2004;16 Suppl 2:21-24.

95. Vedovelli L, Baritussio A, Carnielli VP, Simonato M, Giusti P, Cogo PE. Simultaneous measurement of phosphatidylglycerol and disaturated-phosphatidylcholine palmitate kinetics from alveolar surfactant. Study in infants with stable isotope tracer, coupled with isotope ratio mass spectrometry. *J Mass Spectrom.* Oct 2011;46(10):986-992.

96. Simonato M, Baritussio A, Ori C, et al. Disaturated-phosphatidylcholine and surfactant protein-B turnover in human acute lung injury and in control patients. *Respir Res.* 2011;12:36.

97. Veldhuizen R, Possmayer F. Phospholipid metabolism in lung surfactant. *Subcell Biochem.* 2004;37:359-388.

98. Possmayer F, Yu SH, Weber JM, Harding PG. Pulmonary surfactant. *Can J Biochem Cell Biol.* Nov 1984;62(11):1121-1133.

99. Schmidt R, Meier U, Yabut-Perez M, et al. Alteration of fatty acid profiles in different pulmonary surfactant phospholipids in acute respiratory distress syndrome and severe pneumonia. *Am J Respir Crit Care Med.* Jan 2001;163(1):95-100.

100. Schmidt R, Markart P, Ruppert C, et al. Time-dependent changes in pulmonary surfactant function and composition in acute respiratory distress syndrome due to pneumonia or aspiration. *Respir Res.* 2007;8:55.

101. Girod de Bentzmann S, Pierrot D, Fuchey C, Zahm JM, Morancais JL, Puchelle E. Distearoyl phosphatidylglycerol liposomes improve surface and transport properties of CF mucus. *Eur Respir J.* Sep 1993;6(8):1156-1161.

102. Robertson B, Van Golde LM, Batenburg JJ. *Pulmonary Surfactant: From Molecular Biology to Clinical Practice*. Amsterdam, London, New York, Tokyo: Elsevier Science B.V.; 1992.

103. Van Golde LM, Batenburg JJ, Robertson B. The pulmonary surfactant system: biochemical aspects and functional significance. *Physiol Rev.* Apr 1988;68(2):374-455.

104. Okano G, Sato T, Akino T. Biosynthetic routes of molecular species of lung phosphatidylglycerol. *Tohoku J Exp Med.* Nov 1981;135(3):265-273.

105. Quintero OA, Wright JR. Metabolism of phosphatidylglycerol by alveolar macrophages in vitro. *Am J Physiol Lung Cell Mol Physiol.* Aug 2000;279(2):L399-407.

106. Cogo PE, Gucciardi A, Traldi U, Hilkert AW, Verlato G, Carnielli V. Measurement of pulmonary surfactant disaturated-phosphatidylcholine synthesis in human infants using deuterium incorporation from body water. *J Mass Spectrom.* Jul 2005;40(7):876-881.

107. Torresin M, Zimmermann LJ, Cogo PE, et al. Exogenous surfactant kinetics in infant respiratory distress syndrome: A novel method with stable isotopes. *Am J Respir Crit Care Med.* May 2000;161(5):1584-1589.

108. Bartlett GR. Phosphorus assay in column chromatography. *J Biol Chem.* Mar 1959;234(3):466-468.

109. Egberts J, Bulskool R. Isolation of the acidic phospholipid phosphatidylglycerol from pulmonary surfactant by sorbent extraction chromatography. *Clin Chem.* Jan 1988;34(1):163-164.

110. Fine JB, Sprecher H. Unidimensional thin-layer chromatography of phospholipids on boric acid-impregnated plates. *J Lipid Res.* May 1982;23(4):660-663.

111. Sommerer D, Suss R, Hammerschmidt S, Wirtz H, Arnold K, Schiller J. Analysis of the phospholipid composition of bronchoalveolar lavage (BAL) fluid from man and minipig by MALDI-TOF mass spectrometry in combination with TLC. *J Pharm Biomed Anal.* Apr 1 2004;35(1):199-206.

112. Mason RJ, Nellenbogen J, Clements JA. Isolation of disaturated phosphatidylcholine with osmium tetroxide. *J Lipid Res.* May 1976;17(3):281-284.

113. Touchstone B, Chen JC, Beaver KM. Improved separation of phospholipids in thin layer chromatography. *Lipids.* 1980;15(1):61-62.

114. Carnielli VP, Pederzini F, Vittorangeli R, et al. Plasma and red blood cell fatty acid of very low birth weight infants fed exclusively with expressed preterm human milk. *Pediatr Res.* Apr 1996;39(4 Pt 1):671-679.

115. AOCS. *Official Methods and Recommended Practices of the American Oil Chemists' Society, 4th edn.* Champaign: AOCS Press; 1993.

116. Cogo PE, Facco M, Simonato M, et al. Dosing of porcine surfactant: effect on kinetics and gas exchange in respiratory distress syndrome. *Pediatrics.* Nov 2009;124(5):e950-957.

117. Cogo PE, Toffolo GM, Gucciardi A, Benetazzo A, Cobelli C, Carnielli VP. Surfactant disaturated phosphatidylcholine kinetics in infants with

bronchopulmonary dysplasia measured with stable isotopes and a two-compartment model. *J Appl Physiol.* Jul 2005;99(1):323-329.

118. Cogo PE, Facco M, Simonato M, et al. Pharmacokinetics and clinical predictors of surfactant redosing in respiratory distress syndrome. *Intensive Care Med.* Mar 2011;37(3):510-517.

119. Gucciardi A, Cogo PE, Traldi U, et al. Simplified method for microlitre deuterium measurements in water and urine by gas chromatography-high-temperature conversion-isotope ratio mass spectrometry. *Rapid Commun Mass Spectrom.* Jul 2008;22(13):2097-2103.

120. Bilke S, Mosandl A. Measurements by gas chromatography/pyrolysis/mass spectrometry: fundamental conditions in (2)H/(1)H isotope ratio analysis. *Rapid Commun Mass Spectrom.* 2002;16(5):468-472.

121. Wadke M, Brunengraber H, Lowenstein JM, Dolhun JJ, Arsenault GP. Fatty acid synthesis by liver perfused with deuterated and tritiated water. *Biochemistry.* Jul 3 1973;12(14):2619-2624.

122. Daniels CB, Orgeig S, Smits AW. The Evolution of the Vertebrate Pulmonary Surfactant System. *Physiological Zoology.* 1995;68:539-566.

123. Okano G, Akino T. Changes in the structural and metabolic heterogeneity of phosphatidylcholines in the developing rat lung. *Biochim Biophys Acta.* Mar 30 1978;528(3):373-384.

124. Hallman M, Epstein BL, Gluck L. Analysis of labeling and clearance of lung surfactant phospholipids in rabbit. Evidence of bidirectional surfactant flux between lamellar bodies and alveolar lavage. *J Clin Invest.* Sep 1981;68(3):742-751.

125. Baritussio A, Carraro R, Bellina L, et al. Turnover of phospholipids isolated from fractions of lung lavage fluid. *J Appl Physiol.* Oct 1985;59(4):1055-1060.

126. Bleasdale JE, Thakur NR, Rader GR, Tesan M. Cytidine monophosphate-dependent synthesis of phosphatidylglycerol in permeabilized type II pneumonocytes. *Biochem J.* Dec 1 1985;232(2):539-545.

127. Kuronuma K, Mitsuzawa H, Takeda K, et al. Anionic pulmonary surfactant phospholipids inhibit inflammatory responses from alveolar macrophages and U937 cells by binding the lipopolysaccharide-

interacting proteins CD14 and MD-2. *J Biol Chem.* Sep 18 2009;284(38):25488-25500.

128. Poelma DL, Lachmann B, Haitsma JJ, Zimmermann LJ, van Iwaarden JF. Influence of phosphatidylglycerol on the uptake of liposomes by alveolar cells and on lung function. *J Appl Physiol.* May 2005;98(5):1784-1791.

129. Numata M, Chu HW, Dakhama A, Voelker DR. Pulmonary surfactant phosphatidylglycerol inhibits respiratory syncytial virus-induced inflammation and infection. *Proc Natl Acad Sci U S A.* Jan 5 2010;107(1):320-325.

130. Paschen C, Griese M. Quantitation of surfactant protein B by HPLC in bronchoalveolar lavage fluid. *J Chromatogr B Analyt Technol Biomed Life Sci.* Jan 25 2005;814(2):325-330.

131. Gunther A, Siebert C, Schmidt R, et al. Surfactant alterations in severe pneumonia, acute respiratory distress syndrome, and cardiogenic lung edema. *Am J Respir Crit Care Med.* Jan 1996;153(1):176-184.

132. Baker CS, Evans TW, Randle BJ, Haslam PL. Damage to surfactant-specific protein in acute respiratory distress syndrome. *Lancet.* Apr 10 1999;353(9160):1232-1237.

133. Greene KE, Wright JR, Steinberg KP, et al. Serial changes in surfactant-associated proteins in lung and serum before and after onset of ARDS. *Am J Respir Crit Care Med.* Dec 1999;160(6):1843-1850.

134. Rodriguez-Capote K, Manzanares D, Haines T, Possmayer F. Reactive oxygen species inactivation of surfactant involves structural and functional alterations to surfactant proteins SP-B and SP-C. *Biophys J.* Apr 15 2006;90(8):2808-2821.

135. Frerking I, Gunther A, Seeger W, Pison U. Pulmonary surfactant: functions, abnormalities and therapeutic options. *Intensive Care Med.* Nov 2001;27(11):1699-1717.

136. Taeusch HW, de la Serna JB, Perez-Gil J, Alonso C, Zasadzinski JA. Inactivation of pulmonary surfactant due to serum-inhibited adsorption and reversal by hydrophilic polymers: experimental. *Biophys J.* Sep 2005;89(3):1769-1779.

137. Brash F, Johnen G, Winn-Brash A, et al. Surfactant protein B in Type II Pneumocytes and Intra-Alveolar Surfactant Forms of Human Lungs. *Am J Respir Cell Mol Biol.* 2004;30:449-458.
138. Weaver TE, Conkright JJ. Function of surfactant proteins B and C. *Annu Rev Physiol.* 2001;63:555-578.
139. Zhou L, Lim L, Costa RH, Whitsett J. Thyroid trascription fator-1, hepatocyte nuclear factor-3beta, surfactant protein B, C, and Clara cell secretory protein in developing mouse lung. *The journal of histochemistry and cytochemistry.* 1996;44(10):1183-1193.
140. Hawgood S. Surfactant protein B: structure and function. *Biol Neonate.* 2004;85(4):285-289.
141. Kurutz JW, Lee KY. NMR structure of lung surfactant peptide SP-B(11-25). *Biochemistry.* Jul 30 2002;41(30):9627-9636.
142. Ikegami M, Le Cras TD, Hardie WD, Stahlman MT, Whitsett JA, Korfhagen TR. TGF-alpha perturbs surfactant homeostasis in vivo. *Am J Physiol Lung Cell Mol Physiol.* Jul 2005;289(1):L34-43.
143. Todd DA, Marsh MJ, George A, et al. Surfactant phospholipids, surfactant proteins, and inflammatory markers during acute lung injury in children. *Pediatr Crit Care Med.* Jan 2010;11(1):82-91.
144. Lowry OH, Rosebrough NJ, Farr AL, Randall RJ. Protein measurement with the Folin phenol reagent. *J Biol Chem.* Nov 1951;193(1):265-275.
145. Cogo PE, Giordano G, Badon T, et al. Simultaneous measurement of the rates of appearance of palmitic and linoleic acid in critically ill infants. *Pediatr Res.* Feb 1997;41(2):178-182.
146. Kramer HJ, Schmidt R, Gunther A, Becker G, Suzuki Y, Seeger W. ELISA technique for quantification of surfactant protein B (SP-B) in bronchoalveolar lavage fluid. *Am J Respir Crit Care Med.* Nov 1995;152(5 Pt 1):1540-1544.
147. Baritussio A, Alberti A, Quaglino D, et al. SP-A, SP-B and SP-C in surfactant subtypes around birth: reexamination of alveolar life cycle of surfactant. *Am J Physiol.* 1994;266(4 Pt 1):L436-437.
148. Dargaville PA, South M, Vervaart P, McDougall PN. Validity of markers of dilution in small volume lung lavage. *Am J Respir Crit Care Med.* Sep 1999;160(3):778-784.

149. Corr LT, Berstan R, Evershed RP. Optimisation of derivatisation procedures for the determination of delta13C values of amino acids by gas chromatography/combustion/isotope ratio mass spectrometry. *Rapid Commun Mass Spectrom.* 2007;21(23):3759-3771.

150. Cogo P, Baritussio A, Rosso F, et al. Surfactant-associated protein B kinetics in vivo in newborn infants by stable isotopes. *Pediatr Res.* Apr 2005;57(4):519-522.

151. Husek P. Amino acid derivatization and analysis in five minutes. *FEBS Lett.* Mar 25 1991;280(2):354-356.

152. Nakos G, Kitsiouli EI, Tsangaris I, Lekka ME. Bronchoalveolar lavage fluid characteristics of early intermediate and late phases of ARDS. Alterations in leukocytes, proteins, PAF and surfactant components. *Intensive Care Med.* Apr 1998;24(4):296-303.

153. Epaud R, Ikegami M, Whitsett JA, Jobe AH, Weaver TE, Akinbi HT. Surfactant protein B inhibits endotoxin-induced lung inflammation. *Am J Respir Cell Mol Biol.* Mar 2003;28(3):373-378.

154. Ueda T, Ikegami M, Henry M, Jobe AH. Clearance of surfactant protein B from rabbit lungs. *Am J Physiol.* Apr 1995;268(4 Pt 1):L636-641.

155. Akira S. IL-6-regulated transcription factors. *Int J Biochem Cell Biol.* Dec 1997;29(12):1401-1418.

156. Ikegami M, Falcone A, Whitsett J. STAT-3 regulates surfactant phospholipid homeostasis in normal lung and during endotoxin-mediated lung injury. *J Appl Physiol.* 2008;104:1753-1760.

157. Manzanares D, Rodriguez-Capote K, Liu S, et al. Modification of tryptophan and methionine residues is implicated in the oxidative inactivation of surfactant protein B. *Biochemistry.* May 8 2007;46(18):5604-5615.

158. Glasser SW, Burhans MS, Korfhagen TR, et al. Altered stability of pulmonary surfactant in SP-C-deficient mice. *Proc Natl Acad Sci U S A.* May 22 2001;98(11):6366-6371.

159. Chander A, Johnson RG, Reicherter J, Fisher AB. Lung lamellar bodies maintain an acidic internal pH. *J Biol Chem.* May 5 1986;261(13):6126-6131.

160. Nishi T, Forgac M. The vacuolar (H+)-ATPases--nature's most versatile proton pumps. *Nat Rev Mol Cell Biol.* Feb 2002;3(2):94-103.

161. Finberg KE. The B1-subunit of the H+ ATPase is required for maximal urinary acidification. *Proceedings of the National Academy of Sciences.* 2005;102(38):13616-13621.

162. Miller RL. V-ATPase B1-subunit promoter drives expression of EGFP in intercalated cells of kidney, clear cells of epididymis and airway cells of lung in transgenic mice. *AJP: Cell Physiology.* 2005;288(5):C1134-C1144.

163. Hogan B. *Manipulating the mouse embryo : a laboratory manual*. 2nd ed. Plainview, N.Y.: Cold Spring Harbor Laboratory Press; 1994.

164. Finberg KE, Wagner CA, Stehberger PA, Geibel JP, Lifton RP. Molecular cloning and characterization of Atp6v1b1, the murine vacuolar H+ -ATPase B1-subunit. *Gene.* Oct 30 2003;318:25-34.

165. Da Silva N, Pisitkun T, Belleannee C, et al. Proteomic analysis of V-ATPase-rich cells harvested from the kidney and epididymis by fluorescence-activated cell sorting. *Am J Physiol Cell Physiol.* Jun 2010;298(6):C1326-1342.

166. Paunescu TG, Russo LM, Da Silva N, et al. Compensatory membrane expression of the V-ATPase B2 subunit isoform in renal medullary intercalated cells of B1-deficient mice. *Am J Physiol Renal Physiol.* Dec 2007;293(6):F1915-1926.

167. Sun-Wada GH, Murata Y, Namba M, Yamamoto A, Wada Y, Futai M. Mouse proton pump ATPase C subunit isoforms (C2-a and C2-b) specifically expressed in kidney and lung. *J Biol Chem.* Nov 7 2003;278(45):44843-44851.